Palaeontologia Electronica
palaeo-electronica.org

New Neogene anourosoricin shrews from northern Asia

Vladimir S. Zazhigin and Leonid L. Voyta

ABSTRACT

The shrews of the Anourosoricini tribe (Soricomorpha: Soricidae) were a broadly represented group of the subfamily Soricinae in the Neogene of Palaearctica and show high taxonomic diversity, up to now mostly in Europe. In the current study, the generic diversity of northern Asian anourosoricin is expanded to four: *Crusafontina, Ishimosorex* gen. nov., *Paranourosorex* and *Anourosorex*. Our investigation of original material from 22 Russian and Kazakh localities allowed us to describe fossil material for two endemic northern Asian genera, *Ishimosorex* gen. nov and *Paranourosorex*. Based on the dental features and stratigraphic position, we consider early *Ishimosorex* gen. nov. and later *Paranourosorex* to represent a single evolutionary lineage. The *Ishimosorex-Paranourosorex* lineage existed from the Late Miocene (late Vallesian, MN 10) to early Pliocene (Ruscinian, MN 15) over a broad geographic range in northern Asia from southwestern Siberia to the Inner Mongolia region and consists of five species: *Ishimosorex ishimiensis* gen. et sp. nov., *P. seletiensis, P. inexspectatus, Paranourosorex intermedius* sp. nov. and *P. gigas*.

Vladimir S. Zazhigin. Geological Institute (GIN), Russian Academy of Sciences, Pyzhevskii per. 7, Moscow, 109017, Russia. zazhvol@gmail.com
Leonid L. Voyta. Zoological Institute (ZIN), Russian Academy of Sciences, Universitetskaya nab. 1, Saint Petersburg, 199034, Russia. leonid.voyta@zin.ru

Keywords: Soricidae; Anourosoricini; *Paranourosorex*; *Crusafontina*; *Ishimosorex*; northern Asia; Neogene; new genus; new species

Submission: 15 January 2022. Acceptance: 26 September 2022.

INTRODUCTION

The shrews of Anourosoricini Anderson, 1879 (Soricomorpha: Soricidae), a tribe of the subfamily Soricinae broadly represented in the Neogene of Palaearctica, show high taxonomic diversity mostly in Europe (Rzebik-Kowalska, 1998; van Dam, 2004, 2010; Mészáros, 1997, 1999a, b, 2014; Furió and Agustí, 2017). Presently known Neogene

https://zoobank.org/1726FDAE-2EE5-4145-A124-6D24287C0514

Final citation: Zazhigin, Vladimir S. and Voyta, Leonid L. 2022. New Neogene anourosoricin shrews from northern Asia. Palaeontologia Electronica, 25(3):a29. https://doi.org/10.26879/1209
palaeo-electronica.org/content/2022/3702-neogene-northern-asian-anourosoricini

Asian anourosoricins comprise two genera: *Anourosorex* Milne-Edwards, 1870 (Storch and Qiu, 1991; Storch et al., 1998; Qiu and Storch, 2005) and *Paranourosorex* Rzebik-Kowalska, 1975 (Storch, 1995; Storch and Zazhigin, 1996; Storch et al., 1998; Qiu and Storch, 2000, 2005). Members of *Anourosorex* survive to the present as four separate modern species: *Anourosorex squamipes* Milne-Edwards, 1870, *A. yamashinai* Kuroda, 1935, *A. assamensis* Anderson, 1875 and *A. schmidi* Petter, 1963 (Hutterer, 2005; Burgrin and He, 2018). Extinct members of this genus are represented by four Chinese Pleistocene species, *A. kui* Young and Liu, 1951, *A. edwardsi* Zheng, 1985, *A. qianensis* Zheng, 1985 and *A. triangulatidens* Zheng and Zhang, 1991 (Reumer, 1997; Li et al., 2014), and the Japanese Pleistocene *A. japonicus* Shikama and Hasegwa, 1958, which Storch and Qiu (1991: 611) considered to be closely related to recent *A. squamipes*. Older *Anourosorex oblongus* Storch and Qiu, 1991, is currently known from two late Miocene sites in China, from the type locality Lufeng (Storch and Qiu, 1991; Shihuiba by Qiu and Storch, 2005; MN 11–12) and Leilao (MN 11). New findings of *Anourosorex* (referred to "*Anourosorex*, sp. nov.") are known from the late Miocene Shuitangba site in China (Jablonski et al., 2014). The *Paranourosorex* genus was first described from the early Pliocene Podlesice site in Poland as *Paranourosorex gigas* by Rzebik-Kowalska (1975); however, this genus had a primarily Asian distribution (Storch, 1995; Storch and Zazhigin, 1996; Storch et al., 1998). Its representatives are known from western late Miocene and early Pliocene localities of China (Inner Mongolia), Kazakhstan (northern territories) and Russia (southwestern Siberia) against known *Anourosorex* from eastern China (Storch 1995; Storch and Zazhigin, 1996; Storch et al., 1998; Qiu and Storch, 2000, 2005), with expansion to Europe, where they rarely occurred in Ruscinian faunas (MN 14–15) in Eastern European Plain sites (Agadjanian and Kowalski, 1978; Topachevsky et al., 1988; Agadjanian, 2009) and elsewhere in Eastern Europe (Rzebik-Kowalska, 1975, 1998; Rzebik-Kowalska and Lungu, 2009; Rzebik-Kowalska and Recovets, 2016). At present, three species of *Paranourosorex* have been described: *P. inexspectatus* (Schlosser, 1924), *P. gigas* Rzebik-Kowalska, 1975 and *P. seletiensis* Storch and Zazhigin, 1996. In addition, in the paper by Storch and Zazhigin (1996), two undetermined forms were "*Paranourosorex* sp. 1" from the Kazakh late Miocene Pavlodar 1A site (Turolian, MN 12) and "*Paranourosorex* sp. 2" from two Russian early Pliocene sites, Borki 1A (Ruscinian, MN 14) and Novaya Stanitsa 1A (*ibid*.). The main purpose of the current paper is a reevaluation of the Storch and Zazhigin (1996) material from 22 late Miocene to early Pliocene localities in Russia (southwestern Siberia) and Kazakhstan with a special evaluation of the undetermined forms *Paranourosorex* sp. 1 and *Paranourosorex* sp. 2.

Geological setting. The fossils of Anourosoricini come from 22 late Miocene to early Pliocene sites in southwestern Siberia and northern and northeastern Kazakhstan (Figure 1; Appendix 1): Andreevka (ANR/1A, 2A), Borki 1 (BRK/1A, 1B, 1C), Biteke (BTK), Cherlak 1 (CHR/1A), Isakovka (ISK/1A, 2A), Krasnokutsk (KRN), Kartashovo (KRT), Lezhanka (LZN/1A, 2B), Nizhneil'inka (NIL), Novaya Stanitsa 1 (NST/1A, 1B), Petropavlovsk 1 (PPL/1A), Peshnevo 1 (PSH/1A, 1B), Pavlodar (PVL/1A, 2 'Quarry') and Selety 1 (SLT/1A). These sites were mentioned by Storch and Zazhigin (1996), Storch et al. (1998), Vasilyan et al. (2017), Zazhigin and Voyta (2019). Lithological and biostratigraphic descriptions of the localities have been published in the following articles: Zazhigin and Zykin (1984), Zazhigin (2006), Zykin et al. (1987, 2007) and Zykin (2012).

The 22 localities and their fossiliferous sediments with mammalian remains are attributed to seven regional stratotypic units: the late Miocene Ishim Formation (Zykin, 2012: 188, figure 4.6), late Miocene Pavlodar Formation (Zazhigin and Lopatin, 2001; Zazhigin et al., 2002; Zykin, 2012: 192, figure 4.10), late Miocene Novaya Stanitsa Formation (Zykin, 2012: 209, figure 4.12), late Miocene Rytov Formation (Zykin, 2012: 222), late Miocene Kedey Formation (Zazhigin, 2006), early Pliocene Isakov Formation (Zykin and Zazhigin, 2004; Zykin, 2012: 232, figure 4.13) and early Pliocene Peshnev Formation (Zykin and Zazhigin, 1984; Zykin, 2012: 238). The fossiliferous sediments of Borki/1A are attributed to the Novaya Stanitsa Formation, but the material contained in it probably came (partly at least) from the older underlying layers of the Ishim Formation. Topographically, the BRK/1A sediments lay on Ishim Formation sediments. The sediments of Nizhneil'inka are attributed to the Krutogor Formation (Zykin, 2012: 250), but its material is also probably redeposited from the older underlying layers of the Isakov Formation. In three localities, Biteke, Krasnokutsk and Kartashovo, the fossils were redeposited in Middle–late Pleistocene sediments. For these localities, the regional stratigraphic context is uncertain.

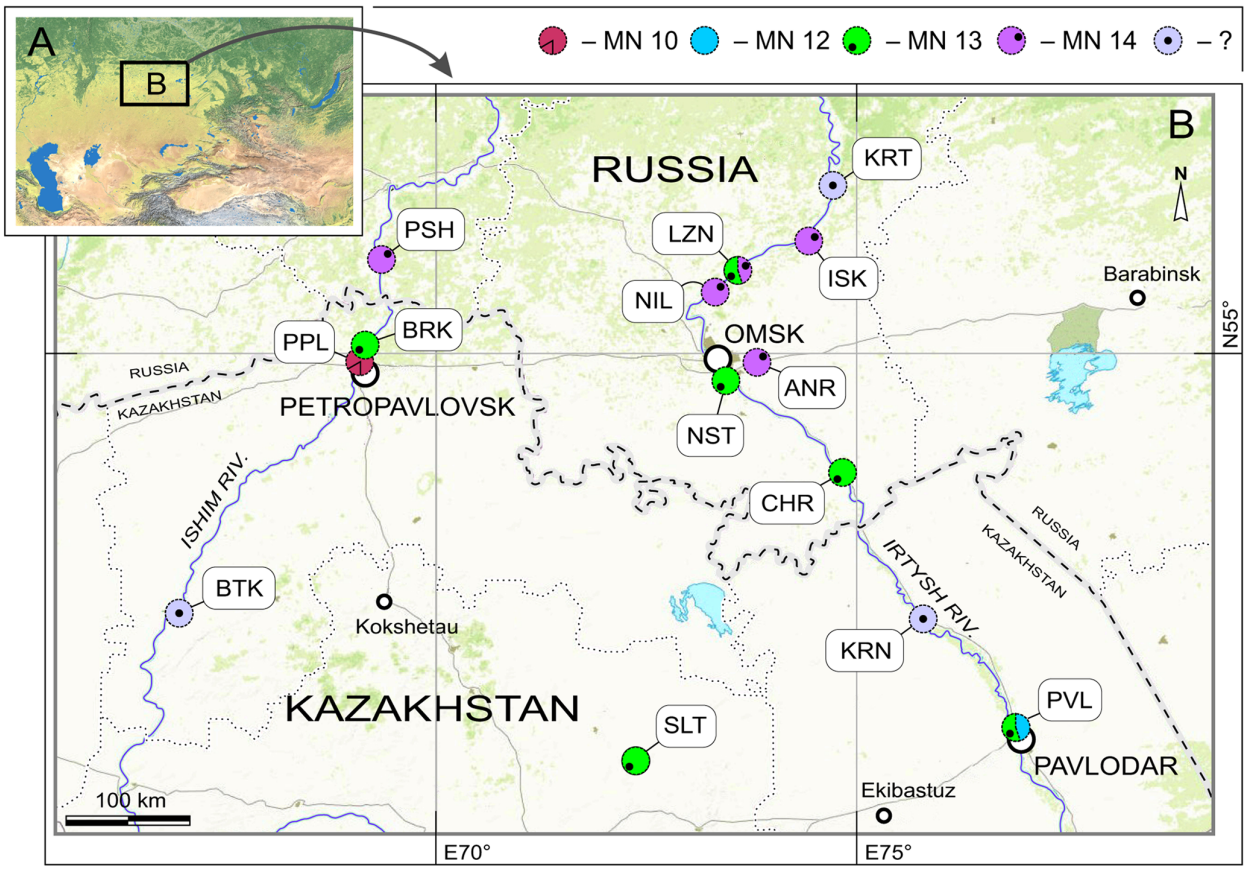

FIGURE 1. Map of Asia (**A**) showing the location of Russian and Kazakh late Miocene and early Pliocene sites (**B**): ANR, Andreevka 1A, 2A; BRK, Borki 1A–C; BTK, Biteke; CHR, Cherlak 1A; ISK, Isakovka 1A, 2A; KRN, Krasnokutsk; KRT, Kartashovo; LZN, Lezhanka 1A, 2B; NIL, Nizhneil'inka; NST, Novaya Stanitsa 1A–B; PPL, Petropavlovsk 1A; PSH, Peshnevo 1A–B; PVL, Pavlodar 1A, 2 'Quarry'; SLT, Selety 1A (type locality of *Paranourosorex seletiensis* Storch and Zazhigin, 1996). Age of the deposits is marked by colours, which corresponds to ELMA Neogene zones 'MN 10, 12–14'; the redeposited fossiliferous layers are marked by '?'. Map data from resource ESRI (http://www.esri.com/) using SASPlanet software (v.160707.9476).

Institutional abbreviations. GIN, Geological Institute of the Russian Academy of Sciences, Moscow; ZIN, Zoological Institute of the Russian Academy of Sciences, St. Petersburg.

MATERIAL AND METHODS

The material of Anourosoricini investigated in this study comprises 184 fossils from 22 late Miocene to early Pliocene localities (Appendix 1). The findings primarily consist of isolated teeth, dentary fragments and rare skull fragments (Appendix 2).

Dental nomenclature follows Reumer (1984), Dannelid (1998) for the general terms and Lopatin (2006: S212) for the special terms of dental cristae and cristids. We do not use the term "W-shaped ectoloph" (Storch, 1995; Storch and Zazhigin, 1996; van Dam, 2004; and others), because we follow to the Lopatin nomenclature, in which the ectoloph compounds only a 'middle part' of the W-shaped line of shrew upper molars. To describe the W-shaped buccal crests of upper molars and its states we must discuss the combined features preparacrista + (postparacrista + premetacrista = centrocrista, ectoloph) + postmetacrista (see Lopatin, 2006: S213). Accordingly, in our description we use 'W-shaped line of upper molar buccal crests.' In a dentition description, we also use two narrowly used terms, 'exaenodonty' and 'dimily.' Exaenodonty is differences between lingual (shorter) and buccal (longer) sides of a tooth base, sense Rich et al. (2001:1). Dimily is tendency to reduce posterior molars, which inherent Dimylidae Schlosser, 1887 (Soricomorpha) and some Soricidae (Heterosoricinae: *Ingentisorex* Hutchison, 1966; Soricinae: *Amblycoptus* Kormos 1926 and *Kordosia*

Mészáros, 1997). The term was introduced by Lopatin (2005: 139).

Pictures of the craniomandibular remains and isolated teeth were taken with a digital camera (Canon EOS 60D) combined with a macro lens (Canon MP-E 65 mm). Features on the images were twice measured with tpsDig ver. 2.31 (Rohlf and Slice, 1990) to minimize 'metering error.' The statistical analysis was performed on the mean values of these replicates. The measurements were mainly taken according to Reumer (1984; for lower teeth) and van Dam (2004; for upper teeth) with some additions (added measurements: HI1c, LBcA1, LLgA1, MRWc, PLi1, RHI1); the measurements are illustrated in Appendix 3. All measurements are given in mm. Calculations were performed in PAST ver. 2.04 and ver. 3.15 (Hammer et al., 2001). The studied taxa measurements are provided in Appendix 4. High-resolution images were acquired using an electronic scanning microscope (Zeiss ESEM Quanta 250), with the surfaces covered by platinum sputter coating; some images were taken by using X-ray computed micro-tomography (NeoScan N80); the images were performed using equipment of the Core Facilities Centre "Taxon" (http://www.ckp-rf.ru/ckp/3038/) of the Zoological Institute of the Russian Academy of Sciences (Saint Petersburg, Russia).

Association of fragmentary findings or 'size recovery' approach. The main problem of the current analysis is the presence of many poor sites with fragmentary remains, which represent a supposed taxon by upper teeth in one site and lower teeth in another site. Because the material should be analysed in view of the synthesis of disparate data on a finite number of known or unknown taxa, we attempted to associate fragmentary remains from different sites. To complete this task, we implemented the Larramendi (2016:539) approach for calculation of a proboscidean shoulder height using dimensions of the known mounted skeletons as references for a determination of ratio between bone lengths within the anatomical position in percents. The author has taken the 'manus height' as 100% and determined the percentages of each bone contribution for different proboscidean taxa. This approach allowed Larramendi (2016) and many others (e.g., Haynes, 2017; Haynes et al., 2018) to use fragmentary skeletal elements (i.e., not associated elements) for the large mammals body size calculation based on a scapula length (scapula-related shoulder height), humerus length (humerus-related shoulder height) or another bone.

We applied the Larramendi strategy to test the association of disparate elements to the same set/taxon as follows:

(a) determining the relationship between particular pairs of the dental and skull elements based on a 'sister' taxon (as reference); where, a 'pair of particular elements' is dictated by the fossils in question (e.g., first upper incisors from Petropavlovsk 1A site vs first lower incisors from Borki 1A site; details see in the main text); the relationship is determined as ratio between longer (100%) and shorter (percents of the longer element) elements. This phase is illustrated in the appendix (Appendix 5: figure 5.1).

(b) 'Size recovering' approach implementation. We divide the matching phase to two steps: (b1) the element size recovery via the accepted ratio of the reference and using a simple formula [(A, mm*REF,%)/100) = B, mm], where, 'A, mm' is an observed measurement of the first anatomic element from one fossiliferous site (Appendix 5: figure 5.2: 'Site AA'); 'REF,%' is reference value for the analysed pair of elements; 'B, mm' is a 'supposed' measurement of the second element from another site (Appendix 5: figure 5.2: 'Site BB'); (b2) matching the 'supposed' and 'observed' (Appendix 5: figure 5.2: 'C, mm') measurements of the second element in mm. We support the association two elements (i.e., they belong to a same set/taxon) when the supposed (recovered) and observed values lay within an allowable interval, which is determined by comparisons to reference set (RST). In this case, RST is any sample with five and more specimens (modern groups) or certainly associated fossils. In the current analysis RST is represented by the samples of *A. squamipes* (n = 17; completed skulls and jaws; ZIN Collection), several pairs of elements of *P. gigas* and *P. seletiensis* (GIN Collection). This phase is illustrated in the appendix (Appendix 5: figure 5.2). Museum numbers of RSTs are provided in the appendix (Appendix 5: table 5.1). Second table (Appendix 5: table 5.2) consists of supposed and observed values for a new species *Ishimosorex ishimiensis* gen. et sp. nov. after the 'size recovering' procedure; observed values in green mark association of the compared anatomic elements, and pink marks dissociation.

SYSTEMATIC PALAEONTOLOGY

Class MAMMALIA Linnaeus, 1758
Order EULIPOTYPHLA Waddell, Okada, and Hasegawa, 1999
Suborder SORICOMORPHA Gregory, 1910
Family SORICIDAE Fischer, 1817
Subfamily SORICINAE Fischer, 1817
Tribe ANOUROSORICINI Anderson, 1879
Genus *ISHIMOSOREX* gen. nov.

zoobank.org/67243F45-1EBF-46CC-A2C7-E6B73680B820

Type species. *Ishimosorex ishimiensis* sp. nov., by monotypy, see below.

Diagnosis. Small-sized anourosoricin shrew. I1 with an elongated and relatively low crown, and short slightly curved root; the hatchet-like (blade-like) talon with expressed narrow, deep notch (like a carnassial notch of lower molars). M1 has a subquadrate occlusal shape with a long and narrow hypoconal flange; the mesostyle is well-developed and protruded buccally; the metaloph is short and separated from the metacone base. i1 with the moderately upturned tip and two slender denticles (bicuspulate) on the cutting edge. p4 has a bulbous-like shape with the round (spot-shaped) wear facet and the very weak expressed central crest; the ecto- and entocingulids are wide and well developed. The hypoconid of m1 and m2 is buccally protruded and overhangs the base of the crown; the entostylid is presented as a small bulge and does not reach the entoconid level by height; entocristid is short. The interarticular area of the condylar process is moderately wide.

Differential diagnosis. *Ishimosorex* gen. nov. differs from *Paranourosorex* in presence of the deep notch and the long crown of I1 and its relatively short root (Figure 2A); in the equal lengths of the lingual and buccal sides of M1; in the deeper posterior emargination of M1 and more posterior protrusion of the hypoconal flange relative the hypocone position (Figure 2G); in presence of two denticles on the cutting edge of i1 and its long medial groove (Figure 3); in the wider interarticular area of the condylar process and the relatively large fossa of the temporal muscle of the mandibular ramus.

Ishimosorex gen. nov. differs from *Crusafontina* in the general proportion of M1 (subsquare vs. trapeziform outline shape), more expressed W-shaped line of the M1 buccal crests, more backwardly protruded the hypoconal flange of M1 (Figure 2G cf. M1 of *C. endemica* from Puente Minero 2, Teruel Basin by van Dam, 2004: figure 2-3); in the slender basal (first) denticle of i1 (Figure 3); in the bulbous-like crown of p4 with the extremely weak expression of the central crest (Figure 4); in a prominent buccal shifting of the protoconid of m1–m2 from the longitudinal axis of the crown and more central position of the entoconid of m1–m2 (*Crusafontina* has a more central position of the protoconid of m1 and a lingually shifted the entoconids of m1–m2 relatively to a basal crown outline; see van Dam, 2004: figure 2).

Ishimosorex gen. nov. differs from *Amblycoptus* and *Kordosia* in the general proportion of I1 with the thin talon (*Amblycoptus* and *Kordosia* both show lateromedial inflation of the talon and expressed bulge of the buccal cingulum); in the proportion and outline shape of M1 (similar to *Crusafontina* buccal crest condition, see above); in the presence of a denticulation of the cutting edge of i1 (Figure 3); in more inflated the anterior part of p4 crown ('subrectangle' shape vs 'subtriangle' shape in *Amblycoptus* and *Kordosia*; Figure 4); in lesser exaenodonty of p4 crown; in a more buccal shifting of the protoconid and hypoconid of m1 from the longitudinal axis of the crown (Figure 2; also see van Dam, 2004: figure 5). The extreme dimily of *Ishimosorex* gen. nov. is doubtful but cannot be test due to lack of data.

Ishimosorex gen. nov. differs from *Darocasorex* in the general proportion of M1 outline shape (*Darocasorex* shows an anteroposterior compression of M1); in absence of the ectocingulid of i1; in absence of expressed crests of p4 (*Darocasorex* has the developed buccal and short lingual crests); in a more longitudinal direction of the oblique crestid of m1 and m2 (see van Dam, 2010).

Ishimosorex gen. nov. differs from *Anourosorex* in the general proportion of I1 and the buccal cingulum condition (*Anourosorex* has a short inflated ectocingulum); in more expressed W-shaped buccal crests and significantly lesser developed of the parastyle of M1 (*Anourosorex* has an extremely developed inflated and buccally protruded parastyle; see Storch and Qiu, 1991); in the bicuspulate i1; in the absence of the expressed and sharp central crest of p4 (*Anourosorex* has very developed, sharp and high central crest); in presence of the ecto- and entocingulids of p4; in the crown proportion of m1–m2 (similar to *Amblycoptus* and *Kordosia* see above).

Etymology. After the Ishim river, located in North Kazakhstan, the provenance of the fossil remains, and from Latin *sorex*, shrew.

Stratigraphic and geographic range. As for the only included species.

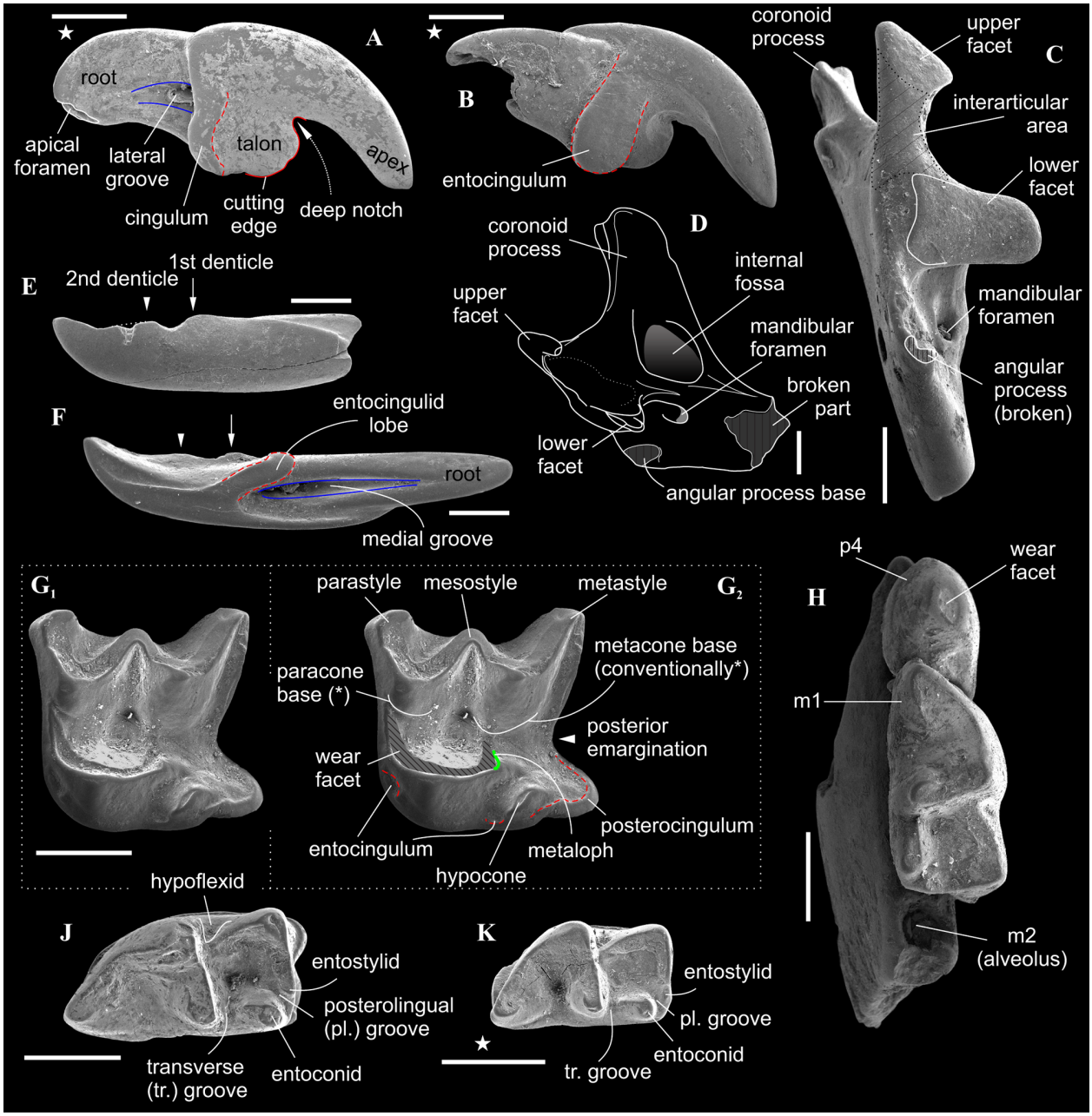

FIGURE 2. Teeth and bones of *Ishimosorex ishimiensis* gen. et sp. nov. from late Miocene Petropavlovsk 1A locality (A–E, G–K) and Borki 1A locality (F). **A**, GIN 952/1161, left I1 in lateral view (Figure 2A cf. Figure 7A); **B**, GIN 952/1160, right I1 in medial view; **C**, GIN 952/1152, left fragment of mandibular ramus in posterior view (image displays articular surface of the condylar process); **D**, *ibid*., diagrammatic image of mandibular ramus in medial view; **E**, GIN 952/1159, left i1 in lateral view; **F**, GIN 1115/1149, right i1 in medial view; **G**, GIN 952/1155, left M1 in occlusal view (**G_1**, pure view; **G_2**, augmented view) (Figure 2G cf. Figure 7H); **H**, GIN 952/1153, right dentary fragment with p4–m1 and anterior alveolus of m2; **J**, GIN 952/1158, right m1 in occlusal view; **K**, GIN 952/1154, left m2 in occlusal view. Star indicates reversed image. Scale bars equal 1 mm.

Ishimosorex ishimiensis sp. nov.
Figure 2

zoobank.org/DFBFD952-8B5C-4392-8522-867F4694C1E1

Type locality. Petropavlovsk 1A, right slope of the Ishim River Valley, within Petropavlovsk town (ca. N54°54' E69°07'), North Kazakhstan Region, Kazakhstan (Figure 1: PPL).

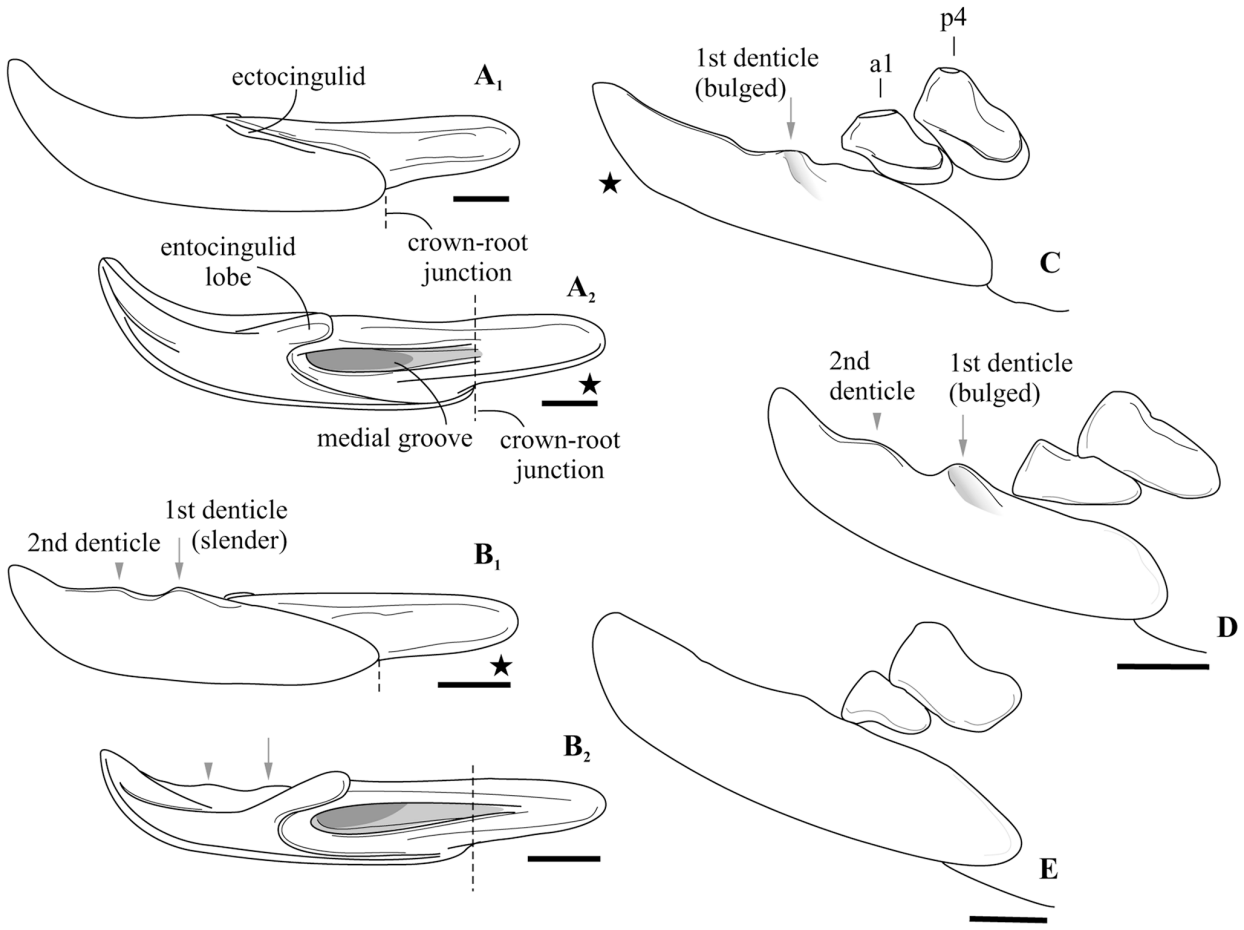

FIGURE 3. The characters of the first lower incisors of *Paranourosorex gigas* from ANR/1A (GIN 1112/1108; $\mathbf{A_1}$, lateral, $\mathbf{A_2}$, medial views), *Ishimosorex ishimiensis* gen. et sp. nov. from BRK/1A (GIN 1115/1149, paratype; $\mathbf{B_1}$, lateral, $\mathbf{B_2}$, medial views), *Crusafontina endemica* Spanish from Can Llobateres 1 locality (**C**, CL1 2217, see van Dam, 2004: 746; in lateral view), *C. kormosi* (**D**, Polgárdi 4, in lateral view) and *A. oligodon* (**E**, Polgárdi 4, in lateral view). Scale bars equal 1 mm; C, unscaled. Abbreviations see in Figure 1.

Type horizon. Stratotypic locality of Ishim Formation (*ish*), late Miocene (MN 10, ?9.7–8.7 Ma). Material was collected by VZ during fieldworks of 1964, 1976, 1980, 1982 and 1987.

Type material. Holotype: GIN 952/1153 — right dentary fragment with p4–m1, the anterior alveolus of m2. Paratypes: (n = 7): GIN 952/1152 — left fragment of mandibular ramus with whole coronoid and condylar processes; GIN 952/1154 — isolated left m2; GIN 952/1055 — isolated left M1; GIN 952/1158 — isolated right m1; GIN 952/1159 — isolated damaged crown part of the left i1; GIN 952/1160 — isolated right I1 with damaged root; GIN 952/1161 — isolated left I1.

Location of types. Holotype and paratypes in the collection of GIN, Moscow (Russia).

Etymology. As for genus name, after the Ishim river.

Material. Type material and four remains from type locality (GIN 952/1157 — damaged right first lower molar; GIN 952/1400 — damaged left P4; GIN 952/1401 — damaged left P4; GIN 952/1402 — damaged left P4); and three rediposited remains (GIN 1115/1148 — worn left I1, crown part; GIN 1115/1149 — right i1; GIN 1115/1150 — left i1) from Borki 1A locality (Appendix 2: 1).

Measurements. See Appendix 4.

Diagnosis. As for genus.

Description. I1 has an elongated massive crown; the large hatchet-like talon bears the sharp cutting edge and expressed narrow, deep notch; the apex of the incisor is not fissident. The buccal cingulum is wide and well expressed without a bulge and reaches half of the crown height. The root is notably shorter and more slender than the crown (Figure 3A, B). Only three damaged fragments of the left P4 without lingual part are known. The buccal

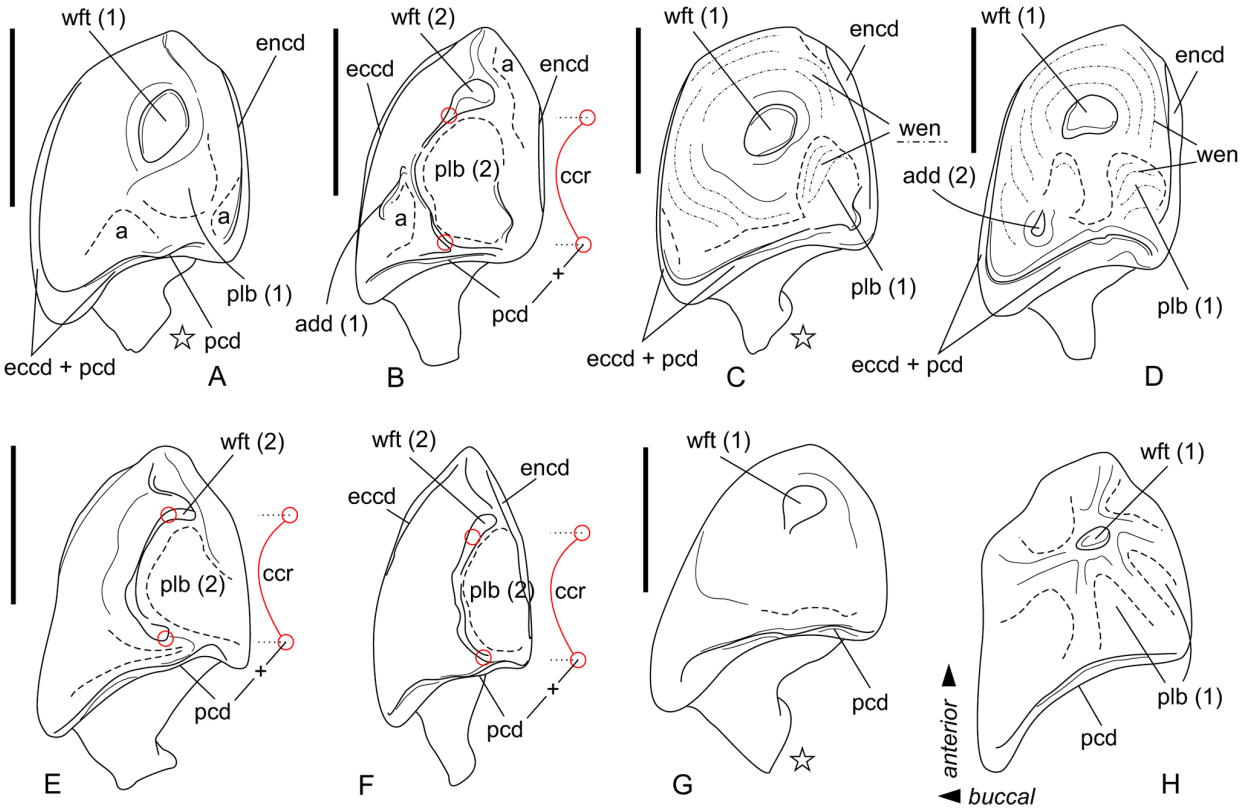

FIGURE 4. Schematic image of the fourth lower premolar of *Ishimosorex ishimiensis* gen. et sp. nov. (**A**, GIN 952/1153, PPL/1A), *Crusafontina kormosi* (**B**, Polgárdi 4), *Paranourosorex intermedius* sp. nov. (**C**, GIN 948/1051, NST/1A), *Paranourosorex gigas* (**D**, GIN 1118/1011, PSH/1B), *Anourosorex squamipes* (**E**, ZIN 98253, Recent), *Crusafontina fastigata* (**F**, AG5A from Los Aguanaces 5A, Teruel Basin, Spain by van Dam, 2004: figs. 4-1), *Amblycoptus oligodon* (**G**, Polgárdi 4) and *Amblycoptus jessiae* (**H**, KS 3157 from Las Casiones, Teruel Basin, Spain by van Dam, 2004: figs. 5-11). Abbreviations: a, concavity; add, additional crown elements (1, crest; 2, cusplet); ccr, central crest; eccd, ectocingulid; encd, entocingulid; pcd, postcingulid; plb, posterolingual basin (1, shallow, weak; 2, expressed); wen, wrinkled enamel; wft, wear facet (1, spot-like; 2, comma-like). Star indicates reversed image. Scale bars are 1 mm; F, H unscaled.

part of these teeth has a relatively short postparacrista; the small parastyle is weakly separated from the paracone base. M1 has a subquadrate occlusal shape with an approximately equal length of the lingual and buccal sides (BL/LL ratio; see Appendix 4); the mesostyle is well-developed and buccally protruded outward of the M1 base level; the buccal crests (preparacrista + ectoloph + postmetacrista) are represented as an expressed W-shaped line; the metaloph is short and separated from the metacone base; the hypocone is rounded distinct cusp and shifted to the lingual margin of the tooth; the weak ridge lays across the hypocone tip obliquely. The posterior emargination of M1 is relatively deep; the hypoconal flange is narrow and elongated backward (Figure 2G). The relative distance between the hypocone and the posterior margin of the flange is distinctly larger than the other taxa have (see comparisons below). The crown of i1 is two times longer than the root (along the lateral side). The medial groove of the root is long and overreaches the crown-root junction. The cutting edge of i1 is bicuspidate; the basal (first) cuspule is slender without any bulge-like expression (opposite state to *Crusafontina*); the distal cuspule is also weak expressed; an ectocingulid is absent (Figure 2E, F). p4 has a massive and rounded crown; the central (single) wear facet is a rounded or 'spot-shaped' (opposite a 'comma-shaped' in *Crisafontina*; see van Dam, 2004: 744). The ecto- and entocingulids are well developed; the ectocindulid continuously passed to postcingulid (Figure 4A). p4 bears a shallow posterolingual basin and extremely weak the central crest, which doesn't reach the postcingulid. The lower molars are graded in size: the first molar is the largest, the second is moderately smaller than the first (Figure 2H–K); the third molar is unknown. The

hypoconid of m1 and m2 is protruded buccally and overhangs the base of the crown; the entostylid is presented as the small distinct bulge and does not reach the entoconid level. The entocristid is short and steeply descends to the metaconid base. The talonid basin opens posterolingually between the entoconid and entostylid through the posterolateral groove and lingually between the end of the entocristid and the metaconid base through the transverse groove. The narrow and well-distinguished ectocingulid does not reach the anterior side of the tooth (Figure 2J, K). The buccal side of m1 has a slightly wrinkled enamel surface. The ectocingulid of m2 is well developed along the tooth base with the plate-like extension in the first third (paraconid level).

The horizontal ramus of the lower jaw is narrow; the small mental foramen is situated slightly backwards of the m1 protoconid level without groove. The mandibular ramus is relatively low; its anterior border is notably tilted backwards. The internal fossa of the temporal muscle ('internal fossa') is moderately developed. The condylar process bears the widely divided upper and lower articular facets and a moderately broad interarticular area (Figure 2C, D).

Association of fragments. The studied remains from PPL/1A were each matched using the size recovery approach and several RSTs, *A. squamipes* and two *Paranourosorex* samples (Appendix 5: tables 5.1 and 5.2) for the following pairs of dental and mandibular elements and measurements: m1/M1: measurements L(m1)/BL(M1); m1/I1: measurements L(m1)/H(I1); I1/i1: measurements L(I1)/L(i1); m1/mandibular ramus: measuremets L(m1)/COR and L(m1)/MRWc. Most of the matched pairs displayed compliance; e.g., the matched m1 and M1 corresponded to each other in size based on the RST ratio. Noncompliance (pink blocks in Table 5.2 of Appendix 5) was revealed for matched upper and lower incisors from PPL/1A (and BRK/1A), i.e., the observed dimension of the lower incisor was less than the supposed dimension calculated based on the *Anourosorex* ratio (Appendix 5: Table 5.1). This noncompliance between calculated and observed incisor sizes could be a specific feature of the particular species, which can be explained in terms allometric heterochrony (sense Mitteroecker et al., 2005: 250). This feature (the ratio between upper and lower incisors) in *Ishimosorex ishimiensis* gen. et sp. nov. differs from *Anourosorex*. In addition, the short lower incisor of *Ishimosorex ishimiensis* gen. et sp. nov. can probably be compensated through a relatively long mandible protraction during a chewing cycle (for details, see below remark on a phenomenon of 'cutting edges straightening'). Proof of this is the best value for the ratio L(m1)/L(i1); i.e., the *Anourosorex* ratio for L(m1)/L(i1) corresponds more to the observed ratio in *Ishimosorex ishimiensis* gen. et sp. nov. than to the ratio L(I1)/L(i1). Thus, the studied remains from PPL/1A can be treated here as belonging to *Ishimosorex ishimiensis* gen. et sp. nov. based on metric matching (Appendix 5: Table 5.2).

Comparisons. *Ishimosorex ishimiensis* gen. et sp. nov. (L(p4) = 1.75 mm; L(m1) = 2.47–2.73 mm, see Appendix 4) differs in larger size from *C. endemica* (L(m1) = 1.90–2.12 mm, see van Dam, 2004: table 4), *Crusafontina exculta* (Mayr and Fahlbusch, 1975) (L(m1) = 1.81–2.21 mm, see Prieto and van Dam, 2012), *Crusafontina fastigata* van Dam, 2004 (L(p4) = 1.43–1.44 mm, ibid.) and *Crusafontina minima* (Hutchinson and Bown, 1980) (L(m1) = 1.77–1.93 mm, see Bown, 1980: table VI). *Ishimosorex ishimiensis* gen. et sp. nov. differs from *Crusafontina vandeweerdi* van Dam, 2004 (L(p4) = 2.24 mm, van Dam, 2004: table 4) in its smaller size. *Ishimosorex ishimiensis* gen. et sp. nov. shows the similar teeth size to *Crusafontina kormosi* (Bachmayer and Wilson, 1970) (L(m1) = 2.38–2.84 mm, see Mészáros, 1998: table 3) and *Crusafontina magna* (Hutchinson and Bown, 1980) (L(m1) = 2.30–2.52 mm, Hutchinson and Bown, 1980: table V) but differs from both species in the well-developed mesostyle of M1, which contrary to *C. kormosi* and *C. magna* shows buccal protrusion of parastyle and metastyle tips (this is also a general difference from *Anourosorex* spp.); in the extremely weak central crest and the spot-shaped wear facet of the p4 opposite well-developed central crest and comma-shaped wear facet of the p4 of *C. kormosi* (Figure 4); p4 of *C. magna* is unknown.

Ishimosorex ishimiensis gen. et sp. nov. differs from *P. seletiensis* in a slightly larger size; from *Paranourosorex intermedius* sp. nov. and *P. gigas* in a distinctly smaller size (Figure 5). *Ishimosorex ishimiensis* gen. et sp. nov. differs from *P. inexspectatus* in a slightly smaller size (Appendix 4). In addition, *Ishimosorex ishimiensis* gen. et sp. nov. morphometrically differs from the known *Paranourosorex* species in longer trigonid of m1 regarding the tooth length (TRL = 62.5% of m1 length) than show *P. seletiensis* (TRL = 57% of m1 length), *Paranourosorex intermedius* sp. nov. (TRL = 56% of m1 length) or *P. gigas* (TRL = 54% of m1 length).

The differences of *Ishimosorex ishimiensis* gen. et sp. nov. from species of *Amblycoptus*, *Kor-*

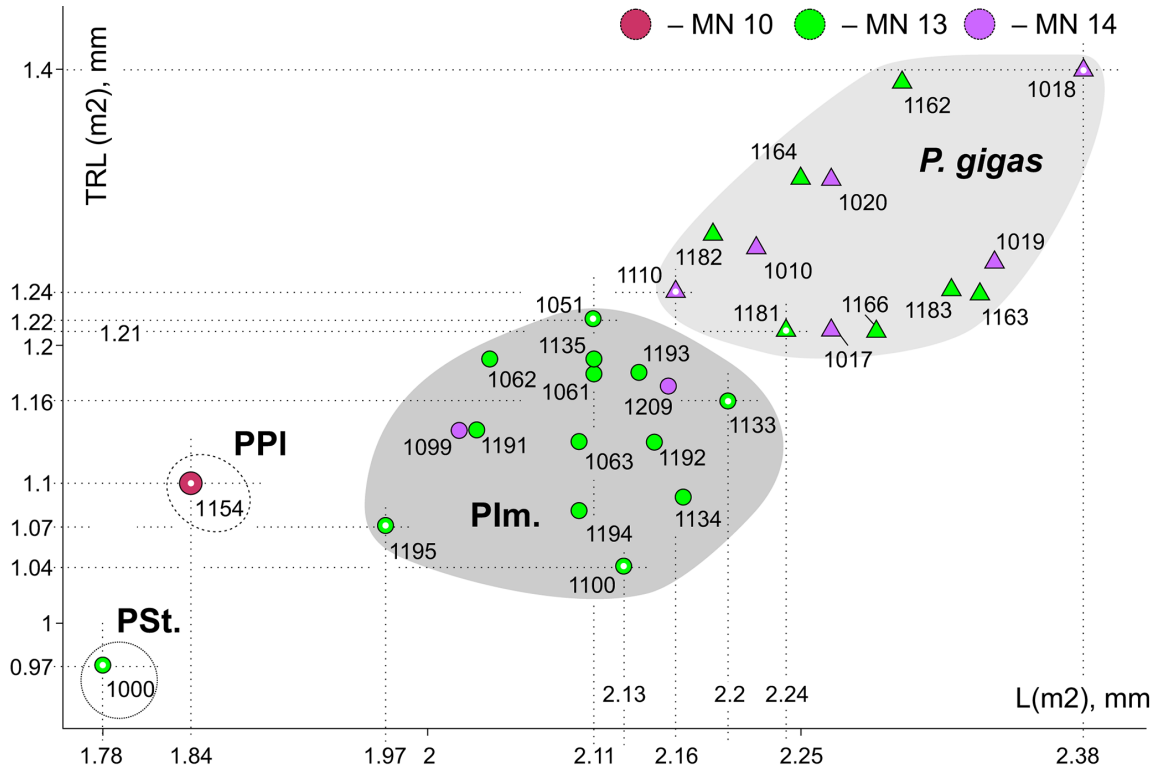

FIGURE 5. Bivariate plot of linear differences between five Asian species, *Paranourosorex seletiensis* Storch and Zazhigin, 1996 (PSt.), *Paranourosorex gigas* Rzebik-Kowalska, 1975 (P. gigas), *Paranourosorex intermedius* sp. nov. (PIm.) and *Ishimosorex ishimiensis* gen. et sp. nov. (PPI) based on the second lower molar measurements (L vs TRL), mm). Studied remains from Asian Neogene localities are marked by colours, which corresponds to ELMA (see Figure 1); numbers are given in the Appendix 2.

dosia and *Darocasorex* were described in the new genus comparisons (see above the Differential Diagnosis section).

Remarks. *Ishimosorex ishimiensis* gen. et sp. nov. shows an intermediate combination of 'omnivorous' features of *Paranourosorex* and 'carnivorous' features of *Crusafontina* in the dentition. M1 bears expressed W-shaped buccal crests and a buccally protruding well-developed mesostyle similar to *Paranourosorex* conditions. In addition, both taxa have a moderately developed parastyle of M1, the bulbous and anteriorly inflated p4 without sharp crests and wide lower molars (buccal shifting of the protoconid and hypoconid). These features are intended for tearing and crushing, i.e., they can be determined as 'omnivore-like features.' In contrast, *Crusafontina* (American and European species, except *C. vandeweerdi*), *Amblycoptus*, *Kordosia* and *Anourosorex* show different degrees of straightening of the buccal crests and increasing (from *Crusafontina* to *Kordosia*) parastyle size of M1. The change in the parastyle together with the trapeziform M1 outline of these taxa probably are related to carnivorous adaptations such as the lengthening of cutting edges; e.g., to the sharp and well-developed central crest of p4 of American and European *Crusafontina*; the central position of the protoconid of m1 and the corresponding lengthening of the preprotocristid of *Crusafontina*, *Amblycoptus*, *Kordosia* and *Anourosorex* to different degrees. Thus, some characteristics of *Ishimosorex ishimiensis* sp. nov. together with *C. vandeweerdi* can be determined as 'carnivore-like' compared with pronounced carnivorous anourosoricins. The deep notch in the talon of I1 and two sharp, slender denticles of the cutting edge of i1 are similar to the American and European species of the more carnivorous *Crusafontina*.

Stratigraphic and geographic range. Known from the type locality of the species (Petropavlovsk 1A, MN 10, Ishim Formation; North Kazakhstan Region) and Borki 1A locality (MN 13, Novaya Stanitsa Formation; North Kazakhstan Region) to which the material was redeposited from Ishim Formation.

Genus *PARANOUROSOREX* Rzebik-Kowalska, 1975

Type species. *Paranourosorex gigas* Rzebik-Kowalska, 1975

Previous diagnosis. Storch and Zazhigin (1996: 259) stated, “Large-sized shrews. Mandibular articulation highly specialized, lower articular facet shifted anteriorly and interarticular area formed by very narrow ridge. P4/4 and M1/1 accentuated, M2/2 and M3/3 reduced. M1/ with W-shaped ectoloph and labially protruding mesostyle, with slight posterior emargination and usually a distinct metaconule. Lower molars with well-developed hypoflexid. P/4 inflated and with strong tendency to reduce the posterolingual basin. Parastyle P4/ protruded anteriorly and protocone shifted lingually. Trigonid on M/1 not particularly elongated. M/1–2 with moderately to weakly developed entocristids. Upper incisor not fissident. Lower incisor with smooth cutting edge. Three upper antemolars and one lower antemolar in front 4th premolar. The teeth are rather bulbous; cingula are well developed. Coronoid process strong and spatulate, with prominent coronoid spicule; internal temporal fossa located anteriorly.”

Emended diagnosis. From small-sized to large-sized shrews. The generalized Anourosoricini dental formula with three upper (A1–A3) and one lower (a1) antemolars and retained third molars (M3 and m3); the dental formula is 1.3.1.3/1.1.1.3. The teeth bear generalized omnivorous characters such as the massive and bulbous-like lower teeth, the hatchet-like talon of I1, the wrinkled enamel on different parts of the teeth, the expressed W-shaped buccal crests line of M1 with well-developed mesostyle, a presence of the short metaloph; the extremely short metastyle (i.e., short postmetacrista) of M2; the wide trigone basin of M1 and trigonid and talonid basins of m1–m2, the well-developed hypoflexid of m1–m2, p4 subrectangle in shape with the spot-shaped wear facet and extremely weak developed the crown structures (central crest and posterolingual basin).

Differential diagnosis. *Paranourosorex* differs from *Crusafontina*, *Amblycoptus*, *Kordosia* and *Anourosorex* in its best developed parastyle of P4 together with a long postcrista; in the mostly expressed W-shaped line of the M1 buccal crests and distinctly buccal protruding of the mesostyle together with the weak developed posterior emargination of P4 and M1 (i.e., a short hypoconal flange); in the subrectangular inflated p4 without developed crown elements and developed ecto- and entocingulids (the compared genera have p4 subtriangle in shape with developed central crista and posterolingual basin in different degree); in the shape of I1 talon (the compared genera have hatchet-like talon with deep notch); in relatively short and wide m1 and m2 (the compared genera have the elongated m1 and m2). In addition, *Paranourosorex* differs from *Crusafontina* in the smooth cutting edge of i1 (Figure 3) and the strongly shorter postmetacrista of M2 together with expressed W-shaped buccal crests of this tooth in general. In addition, *Paranourosorex* differs from *Amblycoptus*, *Kordosia* and *Anourosorex* also in the dental formula composition (*Anourosorex*: 1.2.1.3/1.1.1.3; expressed dimily in *Amblycoptus*: 1.3.1.2/1.1.1.2; and *Kordosia*: 1.2.1.2/1.1.1.2). Differences between *Paranourosorex* and *Ishimosorex* gen. nov. see above. *Paranourosorex* differs from *Darocasorex* in the general proportion of M1 outline shape (*Darocasorex* shows an anteroposterior compression of M1).

Remarks. *Paranourosorex* is probably the Asian origin group that supposedly arose long before the first appearance of *P. seletiensis* in the regional paleontological record. The main evolutionary trend of the genus connects with body size increase of species from early to latter members while maintaining omnivorous, which is marked by basic dental characters adapted for tearing and crushing and consumption of various types of food resources. After the study of Storch and Zazhigin (1996) we revised the available north Asian material and expanded the regional species list for Russia and Kazakhstan to three taxa: *P. seletiensis* Storch and Zazhigin, 1996, *Paranourosorex intermedius* sp. nov. and *P. gigas*.

The Storch and Zazhigin (1996: 259) diagnosis includes several morphological traits that need clarification. A highly specialized craniomandibular articulation is a common character of the tribe. A statement “usually a distinct metaconule” is not entirely accurate; in our interpretation, Anourosoricini has not a true metaconule of M1. Actually, we can see a short metaloph on an unworn tooth. Due to the fact that a metaloph does not reach a metacone base, we observe a metaconule-like bulge on a worn tooth. In addition, the metaloph area of M1 and posterior border of the m1 talonid (hypolophid/entostylid area) shows variations in presence/absence of important characters precisely because these areas are in occlusal contact (Appendix 6) and susceptible to wear.

Stratigraphic and geographic range. At present, the distribution includes 22 localities from Kazakhstan and Russia (Appendix 2) and two European localities (Rzebik-Kowalska, 1975, 1998; Rzebik-Kowalska and Lungu, 2009). The stratigraphic

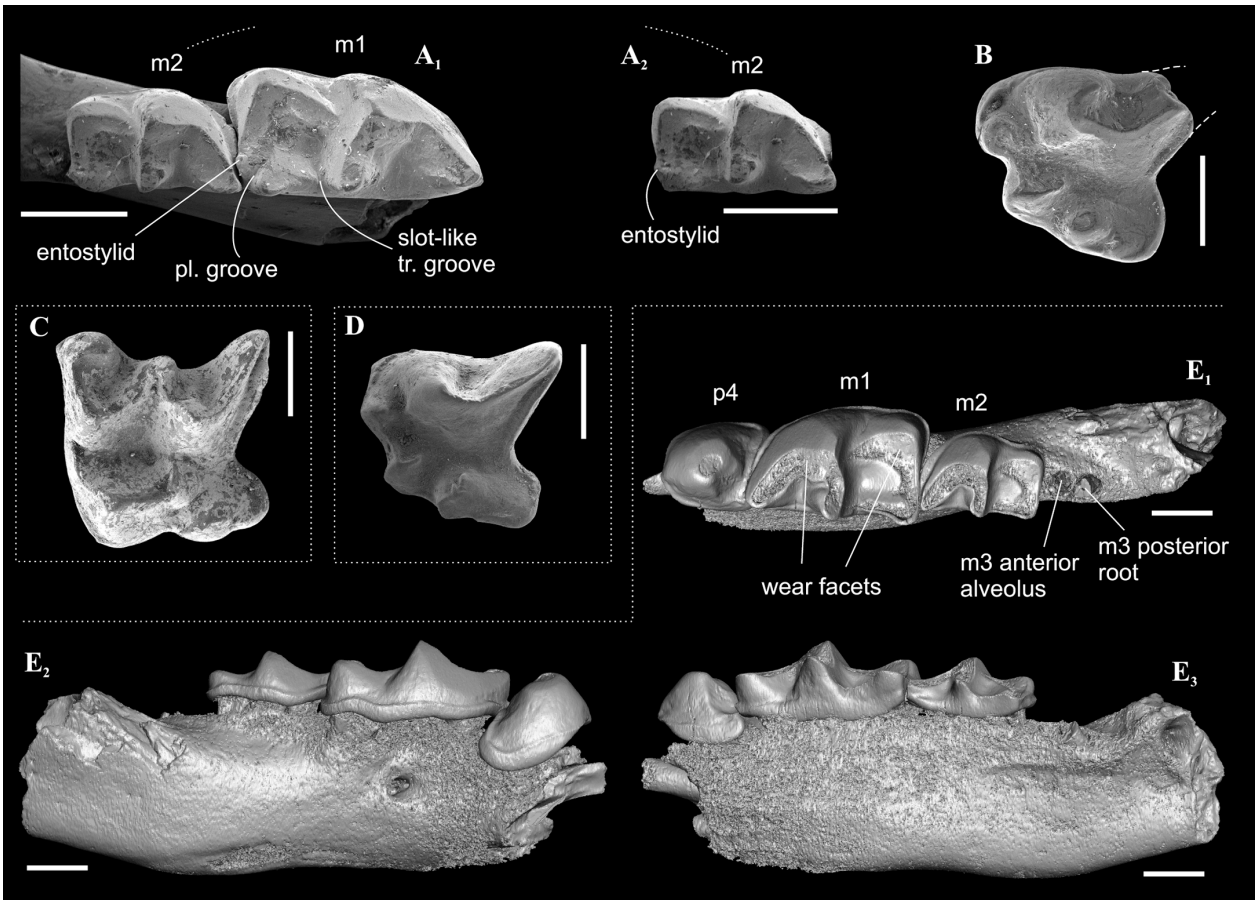

FIGURE 6. Teeth and bones of *Paranourosorex seletiensis* Storch and Zazhigin, 1996 (A, B), *Crusafontina* sp. 1, (C), *Crusafontina* sp. 2 (D) and *Paranourosorex intermedius* sp. nov. (E). **A**, GIN 951/1000 (holotype) from SLT/1A, left hemimandible fragment (cut image) with m1 and m2 in occlusal view (**A_2**, magnified m2); **B**, GIN 951/1001 (paratype) from SLT/1A, left P4 in occlusal view; **C**, GIN 640/1004 from PVL/1A, left M1 in occlusal view; **D**, GIN 951/1003 SLT/1A, left P4 in occlusal view; **E**, GIN 948/1051 (holotype) from NST/1A, right dentary fragment with m1 and m2 (**E_1**, occlusal view; **E_2**, lateral view **E_3**, medial view;). Scale bars equal 1 mm.

range covers an interval between the late Miocene Kedey Formation (Turolian, MN 12/13; Kazakhstan) to early Pliocene (Ruscinian, MN 14, Russia (Peshnev Formation); Ruscinian, MN 15, Slovakia).

Paranourosorex seletiensis Storch and Zazhigin, 1996
Figure 6A, B

Material. Left hemimandible with m1–m2, alveoli of m3 and slightly damaged mandibular ramus without angular process (GIN 951/1000, holotype); isolated left P4 without end of the postparacrista (GIN 951/1001, paratype) from Selety 1A locality. One paratype specimen, isolated right i1 (GIN 951/1002), is lost (Appendix 2: 2).

Description. Smallest *Paranourosorex* species. The general proportion of P4 similar to other *Paranourosorex* species: the moderately developed parastyle is separated from the paracone base by the shallow groove; the well-developed anterior notch between the parastyle and protocone; the well-developed massive cone-like hypocone and the shallow posterior emargination; the parastyle shifts lingually from the paracone longitudinal axis; the postcingulum begins with well-distinguished cingular cuspule (Figure 6B). The hypolophid of m1 ends by the entostylid, which visibly turns backwards; the talonid basin of m1 opens posterolingually by the long posterolingual groove; the entocristid separated from metaconid base by the narrow slot-like transverse groove (Figure 6A). The hypolophid and entoconid of m2 are heavily worn. The lower molars have narrow well-distinguished ectocingulids.

Measurements. See Appendix 4.

Remarks. *P. seletiensis* clearly differs from other *Paranourosorex* species in smallest size (Appendix 4). *P. seletiensis* differs from *P. inexspectatus* (according to the description of Storch, 1995, and Storch and Zazhigin, 1996) and *P. gigas* in the more expressed and turned entostylid of m1; in longer posterolingual groove between the entostylid and entoconid of m1; in presence of the slot-like groove between the entocristid and the metaconid base (other compared species have a wider groove).

Stratigraphic and geographic range. At present, the distribution includes only the type locality (Appendix 2) the late Miocene Kedey Formation (Turolian, MN 12/13).

Paranourosorex intermedius sp. nov.
Figures 6E, 7B, C–D, F–G, I, K, M, O, Q–R

zoobank.org/FA6D006C-2C2A-4860-BE5A-BBAD043A2D49

1996 *Paranourosorex* sp. 2 Storch and Zazhigin, p. 264, figs. 3c, 4l–o.

Type locality. Novaya Stanitsa 1A, right slope of the Irtysh River Valley near Novaya Stanitsa village (ca. N54°50' E73°24'), Omskaya Oblast', Russia (Figure 1: NST).

Type horizon. Stratotypic locality of Novaya Stanitsa Formation (*nst*), late Miocene (Turolian, MN 13). Material was collected by VZ during field-works of 1980s, 2000 and 2001.

Type material. Holotype: GIN 948/1051 — right dentary fragment with moderately worn p4 and heavily worn m1–m3. Paratypes: (n =12): GIN 948/1052 — left dentary fragment with i1, m1 and alveoli of a1–p4 (i1 heavily and m1 moderately worn); GIN 948/1056 — isolated right m1 (slightly worn); GIN 948/1063 — isolated left m2 (slightly worn); GIN 948/1064 — isolated right m3 (slightly worn);GIN 948/1065 — isolated left P4 (slightly worn); GIN 948/1069 — isolated right M1 (metacone damaged; moderately worn); GIN 948/1070 — isolated right M1 (paracone and metacone damaged; moderately worn); GIN 948/1073 — isolated left I1 (slightly worn); GIN 948/1075 — isolated right i1 (tip of root is broken off; moderately worn); GIN 948/1078 — isolated left p4 (without roots; unworn); GIN 948/1081 — isolated left a1 (slightly damaged and worn); GIN 948/1089 — isolated left A1 (slightly worn).

Location of types. Holotype and paratypes in the collection of GIN, Moscow (Russia).

Etymology. From the Latin *intermedius*, intermediate (between smallest *P. seletiensis* and largest *P. gigas*).

Material. Type material and 27 remains from type locality (NST/1A), 60 remains from other 8 localities: NST/1B (n = 1), BRK/1A (n = 26), BRK/1B (n = 18), LZN/2B (n = 8), PVL/2 (n = 1), ISK/1A (n = 1), ISK/2A (n = 3), KRT (n = 1) (see Appendix 2: 3).

Measurements. See Appendix 4.

Diagnosis. Large-sized *Paranourosorex* species. Lower teeth, mostly p4 and m1, are inflated. Upper antemolar row consists of three teeth with vestigial A3. P4 has trapeziform shape with a deep anterior notch and very shallow the posterior emargination. M1 has subquadrate shape with the expressed W-shaped buccal crests, moderately expressed short metaloph without the metacone base contact. p4 is moderately exaenodont, bulbous-like in shape with the spot-shaped wear facet; the posterolingual basin of p4 is very weak. The entocristid of m1 is separated from the metaconid base by a distinctly marked transverse groove; the hypolohid is low; the small entostylid is weakly separated from the entoconid base.

Description. I1 crown proportional in size to the root; the talon has an oblique tilted cutting edge without any notch in the base; the ectocingulum is moderately developed and rises up to the middle of the crown (Figure 7B). The upper antemolars are dramatically decreased in size from the largest A1 to middle-sized A2 (less than 1/2 of A1) and vestigial A3. The addition of cingular cusps (usually one cusp) on the lingual part of the crown is developed on A1; the entocingulum of A2 is smooth. A1 and A2 have developed both anterior and central crests; A1 displays a wrinkled enamel (Figure 7M). P4 has trapeziform crown, developed anterior notch and the shallow posterior emargination. The parastyle is separated from the paracone base by a shallow groove. P4 has a short ectocingulum, well-developed postcingulum and wrinkled enamel on the paracone buccal side (Figure 7C); the entocingulum is absent. M1 has subquadrate occlusal shape with the expressed W-shaped line of the buccal crests. The metaconule is absent; the metaloph is short and separated from the base of the metacone (Figure 7G). The posterior emargination of M1 is shallow. M2 has well-developed cones; the parastyle is longest, the mesostyle is buccally prominent, the metastyle undeveloped; the hypocone round in the base with a spot-shaped wear facet. M3 unknown. i1 has a smooth cutting edge and distinctly upturned tip. The ectocingulid of i1 is undeveloped. The medial groove of the root is short and did not overreach the crown-root junction. a1 has a bulbous-like crown and massive root; the crown with well-developed ecto- and entocin-

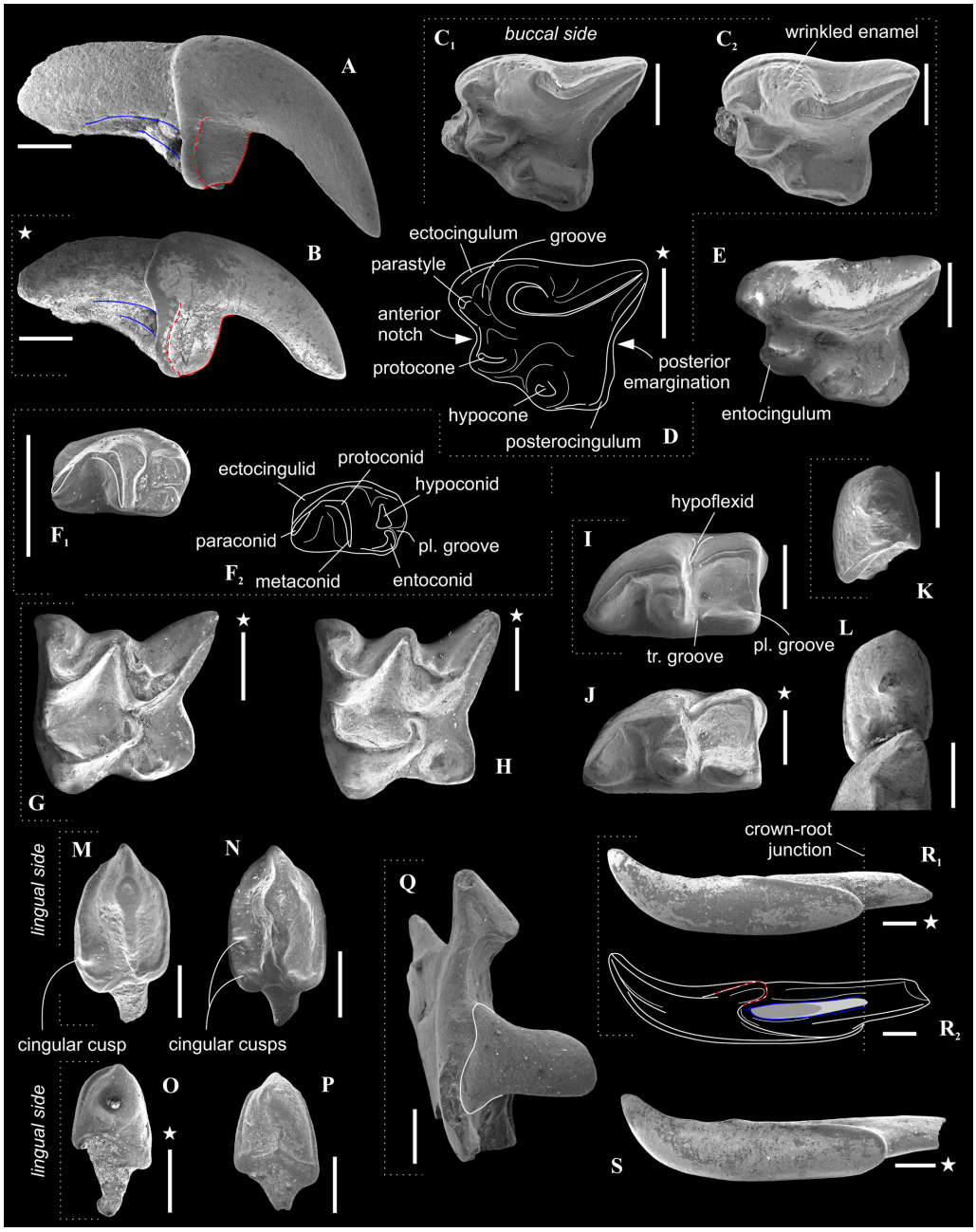

FIGURE 7. Teeth and bones of *Paranourosorex intermedius* sp. nov. (B, C–D, F–G, I, K, M, O, Q–R; with dotted frames) and *Paranourosorex gigas* Rzebik-Kowalska, 1975 (A, E, H, J, L, N, P, S). **A**, GIN 1118/1044 from PSH/1B, right I1 in lateral view; **B**, GIN 948/1073 (paratype) from NST/1A, left I1 in lateral view; **C**, GIN 948/1065 (paratype) from NST/1A, left P4 (**C_1**, occlusal view; **C_2**, tilted occlusal view); **D**, GIN 1130/1104 from LZN/2B, diagrammatic image of right P4 in occlusal view; **E**, GIN 1118/1028 from PSH/1B, left P4 in occlusal view; **F**, GIN 948/1064 (paratype) from NST/1A, right m3 in occlusal view (**F_1**, SEM image; **F_2**, diagrammatic image); **G**, GIN 948/1069 (paratype) from NST/1A, right M1 in occlusal view; **H**, GIN 1118/1005 from PSH/1B, right M1 in occlusal view; **I**, GIN 948/1056 (paratype) from NST/1A, right m1 in occlusal view; **J**, GIN 1118/1013 from PSH/1B, left m1 in occlusal view; **K**, GIN 948/1078 (paratype) from NST/1A, left p4 in occlusal view; **L**, GIN 1118/1011 from PSH/1B, left p4 and m1 fragment (cut image) in occlusal view; **M**, GIN 948/1089 (paratype) from NST/1A, left A1 in occlusal view; **N**, GIN 11181036 from PSH/1B, left A1 in occlusal view; **O**, GIN 948/1081 (paratype) from NST/1A, left a1 in occlusal view; **P**, GIN 1118/1008 from PSH/1B, left a1 in occlusal view; **Q**, GIN 1115/1123 from BRK/1A, left fragment of mandibular ramus in posterior view; **R**, GIN 948/1075 (paratype) from NST/1A, right i1 (**R_1**, SEM image in lateral view; **R_2**, diagrammatic image in medial view); **S**, 1118 951/1021 from PSH/1B, right i1 in lateral view. Scale bars equal 1 mm.

gulids, spot-shaped wear facet and short anterior crest. The central crests of a1 is undeveloped. The inflated p4 bears the spot-shaped wear facet, extremely weak developed the crown structures and distinctly wrinkled enamel (Figures 4C, 7K). m1 is relatively short and wide and so seems slightly inflated. The enamel surface of the trigonid buccal side is slightly wrinkled. The protoconid and metaconid of m1 are brought closer, the hypoconid and entoconid are widely separated. The hypoflexid of m1 is a deep almost vertical groove that does slightly not reach the ectocingulid. The hypolophid is worn in different degrees in all examined specimens, but despite this, we can see two morphotypes: the hypolophid is weakly separated from the entoconid, the entostylid is absent and the posterolingual groove very weak (Morphotype I, GIN 948/1056, NST/1A) (Figure 7I); the hypolophid is clearly separated from the entoconid, the small entostylid and the shallow and short posterolingual groove are present (Morphotype II, GIN 1115/1126, BRK/1B). The entoconid is high and relatively narrow; the entocristid is separated from the metaconid base by a narrow transverse groove. The ectocingulid is well-distinguished along the base of the tooth; entocingulid is absent. m2 notably less than m1; the crown bears the high trigonid and the low talonid. The entostylid is absent; the hypolophid contacts the entoconid without the groove. The entocristid is separated the base of the metaconid by a narrow slot. The ectocingulid m2 is very well-developed along the tooth base with the plate-like extension in the first third (paraconid level). The small m3 has the well-developed trigonid and the reduced talonid without a talonid basin; the talonid consists of the small hypoconid and entoconid that separated by the shallow posterolingual groove (Figure 7F). The ectocingulid of m3 bears the plate-like extension in the first third that is similar to m2.

A single left premaxilla-maxilla fragment with I1 and A2 from PSH/1B (GIN 1118/1027) was examined. I1 is moderately worn; double-rooted A2 is slightly worn. Two alveoli of A1 indicate the presence of the small separated anterior root of A1. Thus, A1 and A2 are both double-rooted.

The mandibular body is long and relatively low without a visible inward curve of the lower outline. The mental foramen is positioned under the protoconid of m1 without any grooves in a wide and shallow depression. The mandibular ramus is massive with a small internal fossa for the temporal muscle; its maximal length is lesser than the condylar height (HC). The coronoid process includes a well-developed long coronoid spicule. The single mandibular foramen is large. The lower articular facet of the condylar process shifts far anteriorly; an interarticular area is relatively narrow (Figure 7Q). An angular process is unknown.

Comparisons. *Paranourosorex intermedius* sp. nov. differs from *P. seletiensis* in a larger size (Figure 5; Appendix 4) and some dental characters (the first species has longer hypoconal flange of P4 and more inflated m1 and m2 than has the second species; Figure 6B cf. Figure 7D). *Paranourosorex intermedius* sp. nov. differs from *P. inexspectatus* in a slightly larger size; in the characters of P4 such as a more developed anterior notch and a more shallow posterior emargination, absent the entocingulum; in a more developed metastyle of M1 (the metastyle of *P. inexspectatus* is relatively shorter and narrower); in a more lingual position of the hypocone and a slightly deeper posterior emargination of M1 (for *P. inexspectatus* see Storch, 1995: plate 4). *Paranourosorex intermedius* sp. nov. differs from *P. gigas* in a slightly smaller size; in a more shallow anterior notch and posterior emargination of P4 (Figure 7: C cf. E); in a more developed metastyle of M1 (the metastyle of *P. gigas* is relatively narrower); in a more lingual position of the hypocone, a slightly longer hypoconal flange and a slightly deeper posterior emargination of M1; in absence of the entocingulum of M1 (Figure 7: G cf. H); in strongly exaenodont buccal half of a1 (Figure 7: O cf. P); in presence of a weak posterolingual groove of m1 (*P. gigas* has not the groove, the hypolophid contacts the entoconid; Morphotype I).

Remarks. The fossils of *Paranourosorex intermedius* sp. nov. correspond to '*Paranourosorex* sp. 2' in Storch and Zazhigin (1996: 264). That description comprises several discordant features that require clarification. Authors stated: "its [p4] apex is weakly two-cusped." We re-evaluated the apex of p4 as a distinctly single cusp with a spot-shaped wear facet (Figure 7K). Authors also stated: "the hypolophid on M/1 is separated from the entoconid by a groove (even in worn specimens)." We found two morphotypes of hypolophid/entoconid of m1 state when the hypolophid is weakly separated from the entoconid with a very weak groove, either the hypolophid is clearly separated from the entoconid with the small entostylid and the shallow and short posterolingual groove.

Much material of *Paranourosorex intermedius* sp. nov. originates from NST/1A (n = 39), BRK/1A (n = 26) and BRK/1B (n = 18). The species is more poorly represented in the other nine sites (Appendix 2). *Paranourosorex intermedius* sp. nov.

probably coexisted with larger shrew *P. gigas* in CHR/1A (Turolian, MN 13, Rytov Formation), ISK/1A (Ruscinian, MN 14, Isakov Formation), PSH/1A and PSH/1B (Ruscinian, MN 14, Peshnev Formation) localities.

Stratigraphic and geographic range. At present, the distribution includes the type locality and 11 localities from Kazakhstan and Russia (Appendix 2) between the late Miocene Novaya Stanitsa Formation (Turolian, MN 13) and the early Pliocene Peshnev Formation (Ruscinian, MN 14).

Paranourosorex gigas Rzebik-Kowalska, 1975
Figure 6A, E, H, J, L, N, P, S

1978 *Crocidura* sp. Agadjanian and Kowalski, p. 33.

1988 *Paranourosorex* sp. Topachevsky et al., p. 20.

2009 Soricidae gen. Agadjanian, p. 102.

Material. The analysed material of *P. gigas* comprises remains mainly from CHR/1A (n = 20) and PSH/1B (n = 33) localities. Single remains originate from ISK/1A (n = 1), NIL (n = 2), PSH/1A (n = 1), ANR/1A (n = 2), ANR/2A (n = 1), LZN/1A (n = 3), BRK/1C (n = 1) and KRN (n = 2) localities (see Appendix 2: 4).

Description. Largest *Paranourosorex* species. In general, the dental characters are typical for the genus but some teeth display specific characters that distinguish this species such as the most undulated and sculptured P4 outline between the parastyle and hypocone with the well-developed anterior notch, the short portion of the entocingulum under the protocone, the moderately developed notch before the hypocone and the protocone lobe; the relatively deep posterior emargination of P4 (Figure 7E); the moderately developed metastyle of M1; the massive cone-like hypocone of M1, relatively short the hypoconal flange and the shallow posterior emargination of M1 (Figure 7H); M1 has a weak entocingulum under the protocone; the moderately exaenodont a1 has a wide postcingulid (Figure 7P); the hypolophid of m1 contacts the entoconid base without a groove; a tip of the entoconid of m1 is slightly shifted anteriorly; the entocristid of m1 is separated from the metaconid base through the moderately developed transverse groove. m3 is unknown.

Measurements. See Appendix 4.

Remarks. *P. gigas* is the biggest species of the tribe, especially in comparison to *P. seletiensis* (Figure 5). To differentiate *P. gigas* from *Paranourosorex intermedius* sp. nov. see above. VZ has seen materials from Obukhovka 1 referred to as '*Paranourosorex* sp.' (Topachevsky et al., 1988); from Antipovka and Chugunovka referred to as '*Crocidura* sp.' by Agadjanian and Kowalski (1978) and 'Soricidae gen.' by Agadjanian (2009) and determined all findings as *P. gigas*.

Much material of *P. gigas* originates from CHR/1A (n = 20) and PSH/1B (n = 33).

Stratigraphic and geographic range. At present, the distribution includes the type locality Podlesice (early Pliocene, Ruscinian, MN 14, Poland), Slovakian locality (early Pliocene, Ruscinian, MN 15) (Rzebik-Kowalska, 1975, 1998), three Eastern European Plain localities such as Obukhovka 1 (Topachevsky et al., 1988), Antipovka and Chugunovka (Agadjanian and Kowalski, 1978; Agadjanian, 2009; early Pliocene, Ruscinian, MN 14) and also 10 localities from Kazakhstan and Russia (Appendix 2). The stratigraphic range in Asia covers an interval between the late Miocene Rytov Formation (Turolian, MN 13) and early Pliocene Peshnev Formation (Ruscinian, MN 14).

Genus *CRUSAFONTINA* Gibert, 1974

Type species. *Crusafontina endemica* Gibert, 1975

1966 *Anourosoricodon* Topachevsky, p. 91. (? nomen oblitum)

1980 *Anouroneomys* Hutchison and Bown in Bown, 1980, p. 105, figs. 2d, 3–6, 7d.

Emended diagnosis. See van Dam (2004).

Remarks. VZ has seen type material of *Anourosoricodon pidoplitschkoi* Topachevsky, 1966 (no. 42-1, a fragment of the right dentary with i1 and m1, and alveoli; see Topachevsky, 1966; Gureev, 1979: 461) from the early Pliocene locality on the left shore of the Kakhovskoie water storage basin near Kamenskoie Village (Ukraine), stored in the Zoological Institute of the Ukraine Academy of Sciences (Kiev, Ukraine) and revealed the conspecifity between *Anourosoricodon* Topachevsky, 1966 and *Crusafontina* Gibert, 1974. Thus, *Anourosoricodon* is the senior synonym. According to Article 23 of ICZN (1999) *Anourosoricodon* is a valid genus name. However, we propose to use point 23.9.3 of ICZN (1999) further refer the matter to the Commission for a ruling under the plenary power with the proposal to use the junior synonym to maintain the stability of the Anourosoricini tribe system because *Crusafontina* name used 47 years and clearly corresponds to particular European taxa and time span. Previously, van Dam (2004: 763) referred to Nesin and Nadachowski (2001) and used *Crusafontina* as a synonym of *Anourosoricodon* without taxonomic remarks.

Type specimen of *Anourosoricodon pidoplitschkoi* corresponds to *C. kormosi* in the i1 and m1 qualitative features and size of m1 (L(m1) = 2.6 mm, see Topachevsky, 1966; Gureev, 1979: 461).

Stratigraphic and geographic range. At present, the distribution includes numerous European localities (Rzebik-Kowalska, 1998; van Dam, 2004), two North American localities (Bown, 1980) and two Asian localities with two undetermined forms, *Crusafontina* sp. 1 (Pavlodar 1A, Kazakhstan) and *Crusafontina* sp. 2 (Selety 1A, Kazakhstan). The stratigraphic range covers an interval between middle Miocene (MN 7/8) to early Pliocene (MN 15) of Europe (see van Dam, 2004: appendix 1); the New World late Miocene late Clarendonian Stage (Juntura Formation) and the early Hemphillian Stage (Ash Hollow Formation; see Bown, 1980); and Asian late Miocene interval restricted by the Turolian Pavlodar (MN 12) and Kedey (MN 12/13) Formations (Kazakhstan).

Crusafontina sp.1
Figure 6C

1996 *Paranourosorex* sp. 1 Storch and Zazhigin, p. 261, fig. 4a.

2004 *Crusafontina*? *vandeweerdi*? van Dam, p. 763.

Material. Isolated left M1 (GIN 640/1004) from Pavlodar 1A locality (Appendix 2: 5).

Description. The large and moderately worn first upper molar displays clearly defined crown features. The buccal crests are expressed W-shaped line like a condition of *Paranourosorex* (Figures 6D cf. 7G). The metaconule is absent; the short metaloph is similar to the *Paranourosorex* condition and has a weak broadening of the base ('poorly developed metaconule' by van Dam 2004: 752) and contacts with the metacone base. The hypocone is elongated in the base and shifts to the lingual margin of the flange. The posterior emargination is well-expressed; the hypoconal flange is protruded posteriorly and narrow in shape.

Measurements. BL(M1) = 2.54 mm; AW(M1) = 2.68 mm; PW(M1) = 2.56 mm; LL(M1) = 2.42 mm; PE(M1) = 2.07 mm (abbr. see in Appendix 3).

Remarks. The M1 is slightly larger than the known M1 of *C. vandeweerdi* (BL = 2.48 mm, AW = 2.58 mm, see van Dam, 2004: 750) and distinctly larger than other species of *Crusafontina*. The crown features of M1 such as the buccal crests shape and the buccal outline are similar to *Paranourosorex* conditions. This fact did not lead Storch and Zazhigin (1996) to determine this molar as a *Crusafontina*. On the other hand, the authors could not associate this molar to *Paranourosorex* without a doubt because it has deep posterior emargination, contact between the metaloph and the base of the metacone and the narrow hypoconal flange. Later, van Dam (2004) supposed the conspecifity of the Pavlodar's form and the new Spanish species *C. vandeweerdi* (Teruel Basin, MN 12), pointed its intermediate feature conditions to both *Crusafontina* and *Paranourosorex*. The species has *Crusafontina*-like p4 with a central crest and distinct posterolingual basin; the ecto- and entocingulids of p4 are absent. We determined the Pavlodar's molar as *Crusafontina* sp. 1 due to the absence of any tooth material for more detailed comparisons with type materials of *C. vandeweerdi*.

Stratigraphic and geographic range. *Crusafontina* sp. 1 known only from the single Kazakh locality, Pavlodar 1A, late Miocene Pavlodar Formation (Turolian, MN 12).

Crusafontina sp. 2
Figure 6D

Material. Isolated left P4 (GIN 951/1003 (1040)) from the Selety 1A locality (Appendix 2: 6).

Description. The small P4 has a strongly undulated and sculptured crown outline between the parastyle and hypocone with a distinguished anterior notch, moderate protrusion of the protocone anteriorly and strong protrusion of the hypocone lingually; the parastyle forms a pointed anterior outline. The parastyle also modestly shifted anteriorly from the paracone base and is separated from it by a groove. The postcrista is relatively short, and tooth seems shortened in general. The hypocone is inflated and seems more massive than the protocone. The hypoconal flange is relatively long and moderately narrow with an angulated posterior outline; the posterior emargination is deep and shifted lingually. The short ectocingulum is present (Figure 6D).

Measurements. BL(P4) = 2.18; W(P4) = 2.06; LL(P4) = 1.76; PE(P4) = 1.41.

Remarks. The studied P4 from the Selety 1A locality is distinctly larger than that from *C. exculta* (BL = 1.97–2.08 mm, see van Dam, 2010: 750) and *C. minima* (BL = 1.84–1.96 mm, see Bown, 1980: 114) and smaller than that from *C. kormosi* (BL = 2.34–2.77 mm, see Mészáros, 1999a: 9) and especially *C. vandeweerdi* (BL mean = 2.72 mm, see van Dam, 2004: 750). This P4 is slightly larger than the P4 of *C. endemica* from European localities (BL = 1.97–2.16 mm, see van Dam, 2004: 750). Initially, we determined the tooth from Selety 1A as belonging to *C. endemica* because it quite precisely fits the crown features and outline of P4 of *C.*

endemica from the Spanish Can Llobateres 1 locality (van Dam, 2004: figure 2:16, but see point 3: 749). However, *C. endemica* is not known in the fossil record later than the end of the Vallesian. Therefore, either *C. endemica* survived in Asia to the beginning of the late Turolian, or we have a tooth of an unknown species of *Crusafontina*. On the other hand, based on the tooth size, outline shape and stratigraphic range, P4 from Selety 1A best matches the New World species *C. magna* (BL = 2.12–2.34 mm; W = 2.15–2.37 mm, see Bown, 1980). Morphologically, P4 from Selety 1A is similar to the tooth of *C. magna* in the distinct anterior projection of the parastyle (with the slight lingual shift from the paracone axis); in the well-developed long notch between the parastyle and protocone and shorter notch between the protocone and huge cone-like hypocone; and in the narrow and posteriorly protruded hypoconal flange with clear cingulum along the border and relatively deep posterior emargination. The poor quality of the Hutchinson and Bown images (Bown, 1980: figure 3A) does not allow us to judge clear similarity in the small crown features. In summary, at present, we determined the tooth from Selety 1A as *Crusafontina* sp. 2 due to the absence of any tooth material for more detailed comparisons with type materials of *C. magna*. In addition, the similarity between P4 from Selety 1A and New World species does not contradict the data on the existence of the Beringian terrestrial bridge during the late Miocene (Wen et al., 2016; Jiang et al., 2019), when *C. magna* could enter Asia from the New World (or vice versa), as Reumer (1999: 393) proposed for Blarinini members.

Stratigraphic and geographic range. At present, the distribution of this form includes only the Kazakh locality, Selety 1A, late Miocene Kedey Formation (Turolian, MN 12/13).

DISCUSSION

Our investigation of original material taken from the Siberian and Kazakh localities revealed the presence of diverse, endemic northern Asian anourosoricin fauna comprising *Ishimosorex* gen. nov. and *Paranourosorex* genus. The new genus has specific features of M1 (expressed W-shaped buccal crests), p4 (an inflated crown, spot-shaped facet and and unexpressed crown elements), m1 (a buccal shift of the protoconid and hypoconid) and m2 (a plate-like ectocingulum), which later appeared in *Paranourosorex*. It is possible that both groups, *Ishimosorex* gen. nov. and *Paranourosorex*, derived from a common ancestor. Therefore, *Ishimosorex-Paranourosorex* lineage existed from the late Miocene (late Vallesian, MN 10) to early Pliocene (Ruscinian, MN 15) within a broad geographic range from southwestern Siberia to the Inner Mongolia region and consisted of five species: *Ishimosorex ishimiensis* gen. et sp. nov., *P. seletiensis*, *P. inexspectatus*, *Paranourosorex intermedius* sp. nov. and *P. gigas*. The latter species expanded to Eastern Europe (Rzebik-Kowalska 1975, 1998).

Northern Asian anourosoricin fauna also included allochthonous elements, which came from Europe and/or North America: two findings of undetermined *Crusafontina* species, namely, *Crusafontina* sp.1 from the Pavlodar 1A locality with similar crown features and dimensions to the late Miocene species *C. vandeweerdi* in Spain, and *Crusafontina* sp.2 from the Selety 1A locality with similar crown features and dimensions to the late Miocene *C. endemica* in Europe or late Miocene *C. magna* in the New World.

In the current study, we find four tendencies in north Asian anourosoricin faunal evolution: (1) the northern Asian endemic *Ishimosorex-Paranourosorex* lineage developed simultaneously or slightly later than the true *Crisafontina* lineage in Europe within the Vallesian Stage (MN 9, 10; see Rzebik-Kowalska, 1998; van Dam, 2004); (2) the first appearance of *Crusafontina* representatives in northern Asian fossil records was associated with the end of the early Turolian Stage (MN 12, MN 12/13). At present, we revealed just two findings of *Crusafontina* from Kazakh localities not later than Kedey Formation deposits (MN 12/13); (3) the evolutionary trajectory of the *Ishimosorex-Paranourosorex* lineage assumed the appearance and disappearance of the earlier *Ishimosorex ishimiensis* gen. et sp. nov. with the further appearance of an earlier *Paranourosorex* species, *P. seletiensis*. The evolutionary lineage of proper *Paranourosorex* species exhibited an increase in overall size from the earlier small-sized form, *P. seletiensis*, to the large-sized form, *P. gigas*. This tendency was already noted by Storch and Zazhigin (1996). We can add a new tendency for this evolutionary lineage, namely the shortening of the related trigonid length of m1 from 62% of the tooth length in *Ishimosorex ishimiensis* gen. et sp. nov. to 54% in *P. gigas*; (4) the *Paranourosorex* species seems to have disappeared in the fossil records with an appearance in Asia of *Beremendia fissidens* (late Ruscinian, MN 15, Biteke Formation; see Zazhigin and Voyta, 2019). This was also mentioned by European authors (Mészáros, 2014: 109, figure 4).

Variability of dental features. The teeth of all studied species of *Paranourosorex* and *Ishimosorex ishimiensis* gen. et sp. nov. display wrinkled enamel. This characteristic of the enamel surface is developed to different degrees and varies within and between species. Wrinkled enamel is most expressed in *Paranourosorex intermedius* sp. nov. (Figure 7C). The most significant variable characteristics are the presence of a metaconule in M1 and the variation in the hypolophid/entostylid states of m1 (I and II morphotypes). We state that the metaconule of M1 was absent in the species of *Ishimosorex-Paranourosorex* lineage. Most likely, this is true for other anourosoricin groups. The review of the metaloph area in *Ishimosorex* gen. nov., *Paranourosorex* and several species of *Crusafontina*, *Amblycoptus* and *Kordosia* revealed different degrees of metaloph development: a short metaloph without contact with the metacone base (Asian taxa) and a long metaloph with weak or expressed contact with the metacone (*C. vandeweerdi*, *A. oligodon*, and *K. topali*). However, some teeth show a metaconule; e.g., van Dam (2004: 752) described *C. vandeweerdi* as "The metaloph shows a 90-degree angle, buccally of which a poorly developed metaconule is present." This is not a true metaconule but rather a partly worn metaloph crest. The selective wear of the metaloph forms by its attrition at the posterior structures of the m1 talonid — the hypoconid-hypolophid-(entostylid)-entoconid line (Appendix 6). We suggest that selective wear is subject to individual variability in relation to different kinds of foods due to various habitats similar to those revealed in other mammalian taxa (e.g., see Smuts et al., 1978 for carnivores; Anders et al., 2011 for artiodactyls) and age variability. Therefore, in well-represented material (e.g., *Paranourosorex intermedius* sp. nov. type locality), we can see the same worn stage of several M1 but different states of the metaloph. The posterior structures of the m1 talonid display similar conditions to the stages of wear of the metaloph. These structures are also subject to variability (individual and age variability). Partly, this is evidenced by the presence of two morphotypes of the entostylid absent/present in m1 of *Paranourosorex intermedius* sp. nov. (see species description). The slightly and moderately worn stages of m1 nevertheless allow us to consider the presence of talonid grooves (posterolingual and transverse) and the presence/absence of entostylid (and its size); consequently, these characteristics are included in species comparisons.

CONCLUSIONS

The shrew tribe Anourosoricini consists of seven genera: *Crusafontina, Darocasorex, Paranourosorex*, *Amblycoptus*, *Kordosia*, *Anourosorex* and *Ishimosorex* gen. nov. In the current study, the generic diversity of northern Asian anourosoricin is expanded from two (Storch et al., 1998) to four genera, *Crusafontina, Ishimosorex* gen. nov., *Paranourosorex* and *Anourosorex*.

We consider *Ishimosorex* gen. nov. and *Paranourosorex* genera as a single evolutionary lineage. The dental analysis of this endemic northern Asian lineage in comparison with other anourosoricin genera revealed a unique combination of ancestral (plesiomorphic) and derived (apomorphic) dental features that were developed within northern Asian genera: ancestral features of M1 (an expressed W-shaped line of the buccal crests), p4 (an inflated crown, spot-shaped facet and poor crown elements), m1 (a buccal shift of the protoconid and hypoconid), and m2 (a plate-like ectocingulum) of *Ishimosorex* gen. nov., which later appeared in *Paranourosorex* species; and derived features of I1 (a talon with an anteriorly tilted cutting edge) and i1 (a smooth cutting edge) of *Paranourosorex*.

In the current paper, we were able to resolve one taxonomic issue of Storch and Zazhigin (1996) with the undetermined form *Paranourosorex* sp. 2, which here was determined to be a new species, *Paranourosorex intermedius* sp. nov. The undetermined *Paranourosorex* sp. 1 of Storch and Zazhigin (1996) is reevaluated to be *Crusafontina* sp. 1. In addition, we revealed a new undetermined form, *Crusafontina* sp. 2 from the Selety 1A locality. Neither species of *Crusafontina* can be resolved without new fossil material.

ACKNOWLEDGEMENTS

Authors are grateful to Dr. Lukács Mészáros for provided access to anourosoricin species from late Miocene Hungarian Polgárdi 4 locality (materials on *Crusafontina kormosi* and *Amblycoptus oligodon* used for composition of Figures 3 and 4 under LM permission) and Dr. Alexey V. Abramov for provided access to materials of the extant *Anourosorex squamipes* (ZIN). Authors also are grateful to three anonymous reviewers who refereed our manuscript and contributing to its improvement. Authors thank Dr. Lars W. Van den Hoek Ostende for help with rare references in Chinese. Authors would like to thank Dr. Marc Furió and Dr. Lu Li for help with translating abstract to Spanish

and Chinese, correspondingly. This study was completed within the framework of the Federal themes of GIN "Paleontological grounds for the stratigraphic scale of the upper Cenozoic of Northern Eurasia" (by Vladimir Zazhigin), and partly funded by Project no. 22-24-00510 of the Russian Scientific Foundation (in parts: data analysis, descriptions, comparisons, text and images creating by Leonid Voyta). The study used the collection materials of the Geological Institute of the Russian Academy of Sciences (Moscow), and Zoological Institute of the Russian Academy of Sciences (St. Petersburg; https://www.ckp-rf.ru/usu/73561/).

REFERENCES

Agadjanian, A.K. 2009. Pliocene-Pleistocene small mammals of the Russian Plain. Nauka, Moscow. (In Russian)

Agadjanian, A.K. and Kowalski, K. 1978. *Prosomys insuliferus* (Kowalski 1958) (Rodentia, Mammalia) from the Oliocene of Poland and of the European Part of the U.S.S.R. Acta Zoologica Cracoviensia, 23:29-53.

Anders, U., von Koenigswald, W., Ruf, I., and Smith, B.H. 2011. Generalized individual dental age stages for fossil and extant placental mammals. Paläontologische Zeitschrift, 85:321-339. https://doi.org/10.1007/s12542-011-0098-9

Bown, T.M. 1980. The fossil Insectivora of Lemoyne Quarry (Ash Hollow Formation, Hemphillian), Keith County, Nebraska. Transactions of the Nebraska Academy of Sciences and Affiliated Scoieties, 8:99-122.

Burgin, C.J. and He, K. 2018. Family Soricidae, p. 332-551. In Wilson, D.E. and Russell, A.M. (eds.), Handbook of the mammals of the world. Vol. 8. Insectivores, sloths and colugos. Lynx Edicions, Barcelona.

Dannelid, E. 1998. Dental adaptations in shrew, p. 157-174. In Wójcik, J.M. and Wolsan, M. (eds.), Evolution of Shrews. Mammal Research Institute Polish Academy of Sciences, Białowieża.

Furió, M. and Augustí, J. 2017. Latest Miocene insectivores from Eastern Spain: Evidence for enhanced latitudinal differences during the Messinian. Geobios, 50:123-140. https://doi.org/10.1016/j.geobios.2017.02.001

Gureev, A.A. 1979. The Fauna of the USSR. Mammals, v. IV, Is. 2. Insectivorous: Hedgehogs, moles, and shrews (Erinaceidae, Talpidae, Soricidae). Izdatel'stvo Nauka, Leningrad. (In Russian)

Hammer, Ø., Harper, D.A.T., and Ryan, P.D. 2001. PAST: Paleontological Statistics software package for and data analysis. Palaeontologia Electronica, 4, 4A:1-9. http://palaeo-electronica.org/2001_1/past/issue1_01.htm.

Haynes, G. 2017. Finding meaning in mammoth age profiles. Quaternary International, 443:65-78. https://doi.org/10.1016/j.quaint.2016.04.012

Haynes, G., Klimowicz, J., and Wojtal, P. 2018. A comparative study of woolly mammoths from the Gravettian site Kraków Spadzista (Poland) based on estimated shoulder heights, demography, and life conditions. Quaternary Research, 90:483-502. https://doi.org/10.1017/qua.2018.60

Hutterer, R. 2005. Order Soricomorpha, p. 220-311. In Wilson, D.E. and Reeder, D.A (eds.), Mammal species of the world: a taxonomical reference. 3rd edition. Vol. 1. Johns Hopkins University Press, Baltimore.

ICZN. 1999. International Code of Zoological Nomenclature. The international Trust for Zoological Nomenclature, London.

Jablonski, N.G., Su, D.F., Flynn, L.J., Ji, X., Deng, C., Kelly, Y., Zhang, Y., Yin, J., You, Y., and Yang, X. 2014. The site of Shuitangba (Yunnan, China) preserves a unique, terminal Miocene fauna. Journal of Vertebrate Paleontology, 34:1251-1257. https://doi.org/10.1080/02724634.2014.843540

Jiang, D., Klaus, S., Zhang, Y.-P., Hillis, D.M., and Li, J.-T. 2019. Asymmetric biotic interchange across the Bering land bridge between Eurasia and North America. National Science Review, 6:739-745. https://doi.org/10.1093/nsr/nwz035

Larramendi, A. 2016. Shoulder height, body mass, and shape of proboscideans. Acta Palaeontologica Polonica, 61:537-574. https://doi.org/10.4202/app.00136.2014

Li, C., Qiu, Z., Tong, Y., Zheng S., and In, X. 2014. Palaeovertebrata Sinica Volume III Basal Synapsids and Mammals Fascicles 3 (Series no.16) Eulipotyphlans, Proteutheres, Chiropterans, Euarchontans, and Anagalids. Science Press, Beijing.

Lopatin, A.V. 2005. Early Paleogene insectivores and modern taxonomic system of Lipotyphla, p. 133-154. In Rozanov, A.Yu., Lopatin, A.V., and Parkhaev, P.Yu. (eds.), A modern palaeontology: Classical and modern methods. Paleontological Institute of the Russian Academy of Sciences, Moscow. (In Russian, with English summary)

Lopatin, A.V. 2006. The origin of shrew family (Soricidae, Mammalia): paleontological data, p. 233-245. In Rozhnov, S.V. (ed.), Evolution of biosphere and biodiversity. KMK Scientific Press Ltd., Moscow. (In Russian)

Mayr, H. and Fahlbusch, V. 1975. Eine unterpliozäne Kleinsäugerfauna aus der Oberen Süßwasser-Molasse Bayerns. Mitteilungen der Bayerischen Staatssamlung für Paläontologie und Historische Geologie, 15:91-111.

Mészáros, L. 1997. *Kordosia*, a new genus for some Late Miocene Amblycoptini shrews (Mammalia, Insectivora). Neues Jahrbuch für Geologie und Paläontologie, Monatshefte, 2:65-78.

Mészáros, L. 1998. Late Miocene Soricidae (Mammalia) fauna from Tardosbánya (Western Hungary). Hantkeniana, 2:103-125.

Mészáros, L. 1999a. An exceptionally rich Soricidae (Mammalia) fauna from the upper Miocene localities of Polgárdi (Hungary). Annales Universitatis Scientiarum Budapestinensis, Sectio Geologica, 32:5-34.

Mészáros, L. 1999b. Some insectivore (Mammalia) remains from the Late Miocene locality of Alsótelekes (Hungary). Annales Universitatis Scientiarum Budapestinensis, Sectio Geologica, 32:35-47.

Mészáros, L. 2014. A possible taphonomical evidence for the palaeoecological role of the giant shrews (Mammalia, Soricidae) in the Carpathian Basin. Hantkeniana, 9:107-116.

Mitteroecker, P., Gunz, P., and Bookstein, F.L. 2005. Heterochrony and geometric morphometrics: a comparison of cranial growth in *Pan paniscus* versus *Pan troglodytes*. Evolution & Development, 7:244-258. https://doi.org/10.1111/j.1525-142x.2005.05027.x

Nesin, V.A. and Nadachowski, A. 2001. Late Miocene and Pliocene small mammal faunas (Insectivora, Lagomorpha, Rodentia) of South-eastern Europe. Acta Zoologica Cracoviensa, 44:107-135.

Prieto, J. and van Dam, J.A. 2012. Primitive Anourosoricini and Allosoricinae from the Miocene of Germany. Geobios, 45:581-589. https://doi.org/10.1016/j.geobios.2012.03.001

Qiu, Z. and Storch, G. 2000. The early Pliocene micromammalian fauna of Bilike, Inner Mongolia, China (Mammalia: Lipotyphla, Chiroptera, Rodentia, Lagomorpha). Senckenbergiana Lethaea, 80:173-229.

Qiu, Z. and Storch, G. 2005. China, p. 37-50. In Hoek Ostende, L.W. van den, Doukas, C.S., and Reumer, J.W.F. (eds.), The fossil record of the Eurasian Neogene insectivores (Erinaceomorpha, Soricomorpha, Mammalia), Part I. Scripta Geologica Special Issue. Leiden.

Reumer, J.W.F. 1984. Ruscinian and Early Pleistocene Soricidae (Insectivora, Mammalia) from Tegelen (The Netherlands) and Hungary. Scripta Geologica, 73:1-173.

Reumer, J.W.F. 1997. De evolutiebiologie van de spitsmuizen (Mammalia, Insectivora, Soricidae). III. De subfamilie Soricinae en het literatuuroverzicht. Cranium, 14:13-36.

Reumer, J.W.F. 1999. Shrews (Mammalia, Insectivora, Soricidae) as paleoclimatic indicators in the European Neogene, p. 390-396. In Agusti, J, Rook, L., and Andrews, P. (eds.), The evolution of Neogene terrestrial ecosystems in Europe, Volume 1: Hominoid evolution and climatic change in Europe. Cambridge University Press, New York.

Rich, T.R., Flannery, T.F., Trusler, P., Kool, L., van Klaveren, N.A., and Vickers-Rich, P. 2001. A second tribosphenic mammal from the Mesozoic of Australia. Records of the Queen Victoria Museum Launceston, 110:1-9.

Rohlf, F.G. and Slice, D.E. 1990. Extension of the Procrustes method for the optimal superimposition of landmarks. Systematic Zoology, 39:40-59. https://doi.org/10.2307/2992207

Rzebik-Kowalska, B. 1975. The Pliocene and Pleistocene insectivores (Mammalia) of Poland. II. Soricidae: *Paranourosorex* and *Amblycoptus*. Acta Zoologica Cracoviensia, 20:167-182.

Rzebik-Kowalska, B. 1998. Fossil history of shrews in Europe, p. 23–92. In Wójcik, J.M. and Wolsan, M. (eds.), Evolution of Shrews. Mammal Research Institute Polish Academy of Sciences, Białowieża.

Rzebik-Kowalska, B. and Lungu, A. 2009. Insectivore mammals from the Late Miocene of the Republic of Moldova. Acta Zoologica Cracoviensia, 52A:11-60.

Rzebik-Kowalska, B. and Rekovets, L.I. 2016. New data on Eulipotyphla (Insectivora, Mammalia) from the Late Miocene to the Middle Pleistocene of Ukraine. Palaeontologia Electronica, 19.1.9A:1-31. https://doi.org/10.26879/573

Smuts, G.L., Anderson, J.L., and Austin, J.C. 1978. Age determination of the African lion (*Panthera leo*). Journal of Zoology, 185:115-146. https://doi.org/10.1111/j.1469-7998.1978.tb03317.x

Storch, G. 1995. The Neogene mammalian faunas of Ertemte and Harr Obo in Inner Mongolia (Nei Mongol), China. — 11. Soricidae (Insectivora). Senckenbergiana Lethaea, 75:221-251.

Storch, G. and Qiu, Z. 1991. Insectivores (Mammalia: Erinaceidae, Soricidae, Talpidae) from the Lufeng hominoid locality, late Miocene, China. Geobios, 24:601-621. https://doi.org/10.1016/0016-6995(91)80025-U

Storch, G. and Zazhigin, V.S. 1996. Taxonomy and phylogeny of the *Paranourosorex* lineage, Neogene of Eurasia (Mammalia: Soricidae: Anourooricini). Paläontologische Zeitschrift, 70:257-268. https://doi.org/10.1007/BF02988282

Storch, G., Qui, Z., and Zazhigin, V.S. 1998. Fossil history of shrews in Asia, p. 93-120. In Wójcik, J.M. and Wolsan, M. (eds.), Evolution of Shrews. Mammal Research Institute Polish Academy of Sciences, Białowieża.

Topachevsky, V.A. 1966. New genus of a large white-toothed shrew (Insectivora, Soricidae) from Pliocene deposits of southern Ukraine, p. 90–96. In Voinctvenski, M.A., Kistjakivski, O.B., Abelentsev, V.I., Sokur, I.T., Gizenko, O.I. and Girenko, L.L. (eds.). Ecology and history of vertebrates of Ukrainian fauna. Naukova Dumka, Kyiv. (In Ukrainian)

Topachevsky, V.A., Nesin, Y.A., Rekovets, L.I., Topachevsky, I.V., and Pashkov, A.V. 1988. A new location of small mammalian remains in Pliocene of the northern Azov Sea area. Dopovidi Akademii Nauk Ukrainskoi RSR, Seria B, 11:18-21. (In Ukrainian)

Van Dam, J.A. 2004. Anourosoricini (Mammalia: Soricidae) from the Mediterranean region: A pre-Quaternary example of recurrent climate-controlled north–south range shifting. Journal of Paleontology, 78:741-764. https://www.jstor.org/stable/4094903

Van Dam, J.A. 2010. The systematic position of Anourosoricini (Soricidae, Mammalia): paleontological and molecular evidence. Journal of Vertebrate Paleontology, 30:1221-1228. https://doi.org/10.1080/02724634.2010.483553

Vasilyan, D., Zazhigin, V.S., and Böhme, M. 2017. Neogene amphibians and reptiles (Caudata, Anura, Gekkota, Lacertilia, and Testudines) from the south of Western Siberia, Russia, and Northeastern Kazakhstan. PeerJ, 5:e3025:1-65. https://doi.org/10.7717/peerj.3025

Wen, J., Nie, Z.-L., and Ickert-Bond, S.M. 2016. Intercontinental disjunctions between eastern Asia and western North America in vascular plants highlight the biogeographic importance of the Bering land bridge from late Cretaceous to Neogene. Journal of Systematics and Evolution, 54:469-490. https://doi.org/10.1111/jse.12222

Zazhigin, V.S. 2006. On fauna of small mammals of the arid zone of south of West Siberia in late Miocene, p. 198–202. In Matishov, G.G. (ed.), Late Cenozoic geological history of the north of the arid zone. YuNC RAN, Rostov-on-Don. (In Russian)

Zazhigin, V.S. and Zykin, V.S. 1984. The new data on the stratigraphy of the Pliocene of the south of West-Siberian Valley, p. 29–53. In Arkhipov, S.A. (ed.), Stratigrafia pogranichnikh otlozhenii neogena i antropogena Sibiri. Institut geologii i geofiziki SO AN SSSR, Novosibirsk. (In Russian)

Zazhigin, V.S. and Lopatin, A.V. 2001. The history of the Dipodoidea (Rodentia, Mammalia) in the Miocene of Asia: 4. Dipodinae at the Miocene-Pliocene Transition. Paleontological Journal, 35:60-74.

Zazhigin, V.S., Lopatin, A.V. and Pokatilov, A.G. 2002. The history of the Dipodidae (Rodentia, Mammalia) in the Miocene of Asia: 5. Lophocricetus (Lophocricetinae). Paleontological Journal, 36:180-194.

Zazhigin, V.S. and Voyta, L.L. 2019. Northern Asian Pliocene–Pleistocene beremendiin shrews (Mammalia, Lipotyphla, Soricidae): a description of material from Russia (Siberia), Kazakhstan, and Mongolia and the paleobiology of Beremendia. Journal of Paleontology, 93:1234-1257. https://doi.org/10.1017/jpa.2019.51

Zykin, V.S. 2012. Stratigraphy and evolution of environments and climate during Late Cenozoic in the Southern West Siberia. Academic Publishing House “Geo”, Novosibirsk. (In Russian)
Zykin, V.S. and Zazhigin, V.S. 1984. On determination of the Peshnev Formation in Pliocene of south of West-Siberian Plain. Geology and Geophysics, 2:46-50. (In Russian)
Zykin, V.S., Zazhigin, V.S., and Presyazhnjuk, V.A. 1987. Stratigraphy of Pliocene and Eopleistocene deposits from the Biteke river valley (Northern Kazakhstan). Geologia i Stratigrafia, 3:12-19. (In Russian)
Zykin, V.S. and Zazhigin, V.S. 2004. A new biostratigraphic level of Pliocene of West Siberia and age of the lower–middle Miocene Besheul horyzon stratotipic age. Doklady Akademii Nauk, 398:214-217. (In Russian)
Zykin, V.S., Zykina, V.S., and Zazhigin, V.S. 2007. Issue in separating and correlating Pliocene and Quaternary sediments of Southwestern Siberia. Archeology, Ethnology & Anthropology of Eurasia, 2(30):24–40.

APPENDICES

APPENDIX 1. LIST OF LOCALITIES

Information is in the following order: full name of a locality (bolded), abbreviation in parentheses (bolded; abbreviation used in text and for all Figs and Tabs), age attribution and name of a regional stratotype (= formation), collector and collecting year, geographic position. References see on the bottom.

North Kazakhstan

1. **Petropavlovsk 1A (PPL/1A):** late Miocene, MN 10, Ishim Formation, *ish* (stratotype); material collected by Vladimir S. Zazhigin, 1964, 1976, 1980, 1982, 1987; North Kazakhstan Region, Kazakhstan (ca. N54°54' E69°07').

2. **Pavlodar 1A (PVL/1A):** late Miocene, MN 12, Pavlodar Formation, *pv* (stratotype); material collected by Vladimir S. Zazhigin; Pavlodarskaya Oblast', Kazakhstan (ca. N52°16' E77°01'). Synonym of the 'Gusinyi Perelet' locality ('Goose flight').

3. **Pavlodar 2, Quarry (PVL/2):** late Miocene, MN 13, Rytov Formation, *rt*; material collected by Vladimir S. Zazhigin; *ibid*.

4. **Selety 1A (SLT/1A):** late Miocene, MN 13, Kedey Formation, *kd*; material collected by Vladimir S. Zazhigin; Akmolinskaya Oblast', Kazakhstan (ca. N52°06' E72°21').

5. **Borki 1A (BRK/1A):** late Miocene, MN 13, Novaya Stanitsa Formation, *nst*; material collected by Vladimir S. Zazhigin; a material probably redeposited from Ishim Formation; North Kazakhstan Region, Kazakhstan (ca. N54°56' E69°07').

6. **Borki 1B (BRK/1B):** late Miocene, MN 13, Rytov Formation, *rt*; material collected by Vladimir S. Zazhigin; *ibid*.

7. **Borki 1C (BRK/1C):** early Pliocene, MN 14, Peshnev Formation, *psh*; material collected by Vladimir S. Zazhigin, 1985; *ibid*.

8. **Krasnokutsk (KRN):** age undetermined; sediments redeposited; material collected by Vladimir S. Zazhigin; a material redeposited in Late Pleistocene layers; Pavlodarskaya Oblast', Kazakhstan (ca. N53°00′ E75°58′).

9. **Biteke (BTK):** age undetermined (~ early Pliocene, Kuskol Formation); sediments redeposited; material collected by Vladimir S. Zazhigin; a material redeposited in Biteke Formation; Kostanaiskaya Oblast', Kazakhstan (ca. N53°12' E66°58').

South-West Siberia

10. **Novaya Stanitsa 1A (NST/1A):** late Miocene, MN 13, Novaya Stanitsa Formation, *nst* (stratotype); basal level; material collected by Vladimir S. Zazhigin, 80s, 2000, 2001; Omskaya Oblast', Russia (ca. N54°50' E73°24').

11. **Novaya Stanitsa 1B (NST/1B):** late Miocene, MN 13, Novaya Stanitsa Formation, *nst*; gravel with Unio; material collected by Vladimir S. Zazhigin; *ibid*.

12. **Lezhanka 1A (LZN/1A):** late Miocene, MN 14, Peshnev Formation, *psh*; material collected by Vladimir S. Zazhigin; Omskaya Oblast', Russia (ca. N55°27′ E73°26′); the left slope of Faddeevsky Log (ravine).

13. **Lezhanka 2B (LZN/2B):** late Miocene, MN 13, Rytov Formation, *rt*; material collected by Vladimir S. Zazhigin; ibid.; the mouth of Faddeevsky Log (ravine).

14. **Cherlak 1A (CHR/1A):** late Miocene, MN 13, Rytov Formation, *rt*; basal level; material collected by Vladimir S. Zazhigin, 80th, 2008; Omskaya Oblast', Russia (ca. N54°09′ E74°48′).

15. **Isakovka 1A (ISK/1A):** early Pliocene, MN 14, Isakov Formation (basal level), *is*; material collected by Vladimir S. Zazhigin; Omskaya Oblast', Russia (ca. N55°44' E74°24').

16. **Isakovka 2A (ISK/2A):** early Pliocene, MN 14, Isakov Formation (basal level), *is*; material collected by Vladimir S. Zazhigin; *ibid*.
Note: syn. 'Iskakova' locality by Vasilyan et al. (2017).

17. **Peshnevo 1A (PSH/1A):** early Pliocene, MN 14, Peshnev Formation, *psh*; material collected by Vladimir S. Zazhigin, 1981, 1982, 1989; Tumenskaya Oblast', Russia (ca. N55°33' E69°24').

18. **Peshnevo 1B (PSH/1B):** early Pliocene, MN 14, Peshnev Formation, *psh*; upper fossiliferous level; material collected by Vladimir S. Zazhigin, 1982, 1989; *ibid*. Synonym of the 'Peshniovo' locality by Vasilyan et al. (2017).

19. **Andreevka 1A (ANR/1A):** early Pliocene, MN 14, Peshnev Formation, *psh*; material collected by Vladimir S. Zazhigin, 1992; Omskaya Oblast', Russia (ca. N55°02' E73°36'); 'ravine with flora'.

20. **Andreevka 2A (ANR/2A)**: early Pliocene, MN 14, Peshnev Formation, *psh*; material collected by Vladimir S. Zazhigin; Omskaya Oblast', Russia (ca. N55°02' E73°36').

21. **Nizhneil'inka (NIL):** Omskaya Oblast', Russia (ca. N55°22' E73°14'); early Pliocene, MN 14, Krutogor Formation, *krt*; material collected by Vladimir S. Zazhigin; basal level of Krutogor Formation; a material probably redeposited from Isakov Formation.

22. **Kartashovo (KRT):** Omskaya Oblast', Russia (ca. N56°06' E74°44'); age undetermined; sediments redeposited; material collected by Vladimir S. Zazhigin, 1965.

APPENDIX 2. LIST OF ANALYZED FOSSIL SPECIMENS

Information is in the following order: abbreviation of the locality (bolded; detail see in Appendix 1), number of specimens in parenthesis, number of the collection catalogue of the Geological Institute of the Russian Academy of Sciences, Moscow (bolded), short description of specimen.

1. ***Ishimosorex ishimiensis* gen. et sp. nov.** (n = 16): **PPL/1A** (n = 9): **GIN 952/1153** (holotype) — right dentary fragment with p4–m1, the anterior alveolus of m2; **Paratypes** (n = 8): **GIN 952/1152** — left fragment of mandibular ramus with whole coronoid and condylar processes; **/1154** — isolated left lower second molar; **/1155** — isolated left first upper molar; **/1157** — damaged right first lower molar; **/1158** — isolated right first lower molar; **/1159** — isolated damaged crown part of the left first lower incisor; **/1160** — isolated right first upper incisor with damaged root; **/1161** — isolated left first upper incisor; **Other material** (n = 4): **GIN 952/1157** — damaged right first lower molar; **/1400** — damaged left P4; **/1401** — damaged left P4; **/1402** — damaged left P4.

BRK/1A (n = 3): **GIN 1115/1148** — worn left I1, crown part; **/1149** — right i1; **/1150** — left i1.

2. ***Paranourosorex seletiensis* Storch and Zazhigin, 1996** (n = 2): **SLT/1A, type locality** (n = 2): **GIN 951/1000 (1038**) (holotype) — left dentary fragment with m1–m2, alveoli of m3 and slightly damaged mandibular ramus without angular process; **Paratypes**: (n = 1): **GIN 951/1001(1039)** — isolated left P4 without

end of the postparacrista.

3. ***Paranourosorex intermedius* sp. nov.** (n = 98): **NST/1A, type locality** (n = 39): **GIN 948/1051** (holotype) — right dentary fragment with moderately worn p4 and heavily worn m1–m3; **Paratypes**: (n = 12): **GIN 948/1052** — left dentary fragment with i1, m1 and alveoli of a1–p4 (i1 heavily and m1 moderately worn); **/1056** — isolated right first lower molar (slightly worn); **/1063** — isolated left m2 (slightly worn); **/1064** — isolated right m3 (slightly worn); **/1065** — isolated left fourth upper premolar (slightly worn); **/1069** — isolated right first upper molar (metacone damaged; moderately worn); **/1070** — isolated right first upper molar (paracone and metacone damaged; moderately worn); **/1073** — isolated left first upper incisive (slightly worn); **/1075** — isolated right first lower incisive (tip of root is broken off; moderately worn); **/1078** — isolated left fourth lower premolar (without roots; unworn); **/1081** — isolated left first lower antemolar (slightly damaged and worn); **/1089** — isolated left first upper antemolar (slightly worn). **Other material** (n = 26): **GIN 948/1053** — right mandibular ramus fragment with damaged coronoid and angular processes; **/1054** — isolated left m1 (heavily worn); **/1055** — isolated left m1; **/1057** — isolated right m1; **/1058** — isolated right m1; **/1059** — isolated left m1 (damaged); **/1060** — isolated left m1 (damaged); **/1061** — isolated right m2 (damaged); **/1062** — isolated left m2 (damaged); **/1066** — isolated left P4 (slightly worn); **/1067** — isolated right M1 (heavily worn); **/1072** — damaged right M2; **/1076** — crown part of the left i1; **/1077** — damaged right i1 without the crown tip; **/1079** — isolated left p4 without roots; **/1080** — isolated left p4 without roots; **/1082** — isolated left a1 without roots (damaged); **/1083** — isolated left a1 without roots (damaged); **/1084** — isolated right a1 without roots (damaged); **/1086** — isolated right A3; **/1087** — isolated right A1 (damaged); **/1088** — isolated right A1 without roots; **/1090** — isolated left A1; **/1091** — isolated right A1 without roots; **/1093** — isolated right A2; **/1095** — isolated right A2.

NST/1B (n = 1): **GIN 948/1097** — isolated right P4.

BRK/1A (n = 26): **GIN 1115/1121** — left dentary fragment with talonid m1, m2, alveoli of m3 and damaged mandibular ramus (coronoid process is broken, lower facet of condylar process is retained); **/1122** — left edentulous dentary fragment with alveoli of m2–m3, whole coronoid process and slightly rounded condylar process (upper facet damaged); **/1123** — left mandibular ramus fragment with whole coronoid and slightly damaged condylar process; **/1124** — right dentary fragment with p4–m1 (slightly worn); **/1125** — left dentary fragment with p4–m1 (buccal half of p4 retained); **/1126** — isolated left m1; **/1127** — right damaged m1 on a small dentary fragment; **/1128** — isolated right m1; **/1129** — left damaged m1; **/1130** — left damaged m1 on the small dentary fragment; **/1131** — left damaged m1; **/1132** — left damaged m1; **/1133** — isolated left m2; **/1134** — isolated left m2 (heavily worn); **/1135** — right damaged m2; **/1136** — isolated right M1 without parastyle; **/1137** — isolated left M1 without para- and metastyles; **/1138** — isolated right M1; **/1139** — isolated left M1; **/1140** — isolated right M2 without parastyle; **/1141** — isolated right M2 without para- and metastyles; **/1142** — isolated left A1 with damager crown; **/1143** — isolated left A1; **/1144** — isolated right A1 with damager crown; **/1147** — isolated left a1 without roots; **/1151** — crown of the left i1.

BRK/1B (n = 18): **GIN 1115/1186** — right dentary fragment with m1 and alveoli of a1, p4, m2, m3; **/1187** — isolated right m1 (damaged); **/1188** — isolated right m1 (damaged); **/1189** — isolated right m1 (damaged); **/1190** — isolated left m1; **/1191** — isolated right m2; **/1192** — isolated right m2 (damaged); **/1193** — isolated left m2 (damaged); **/1194** — isolated left m2 (heavily worn); **/1195** — isolated right m2 (damaged); /**1196** — crown of left I1; **/1198** — isolated left M1; **/1199** — damaged left P4; **/1200** — damaged left M1; **/120**1 — damaged right M1; **/1202** — damaged left M2; **/1203** — isolated right i1; **/1204** — isolated right i1.

LZN/2B (n = 8): **GIN 1130/1098** — isolated right m1; **/1099** — isolated right m2; **/1100** — isolated right m2; **/1101** — isolated right m3; **/1102** — isolated left p4 without roots; **/1103** — isolated left a1; **/1104** — isolated right P4; **/1105** — damaged left M2.

PVL/2 (n = 1): **GIN 1108/1106** — left dentary fragment with m1 and alveoli of a1, p4, m2.

ISK/1A (n = 1): **GIN 1113/1209** — isolated left m2.

ISK/2A (n = 3): **GIN 1113/1205** — isolated left m1; **/1206** — damaged right A1; **/1207** — isolated left A2 without root/

KRT (n = 1): **GIN 949/1118** — right small fragment of maxilla with P4 and alveoli of A2, A3.

4. ***Paranourosorex gigas*** **Rzebik-Kowalska, 1975** (n = 66): **CHR/1A** (n = 20): **GIN 1110/1162** — right dentary fragment with m1–m2 and alveoli of p4 and m3; **/1163** — left dentary fragment with p4–m2; **/1164** — right dentary fragment with i1, p4–m2; **/1165** — left dentary small fragment with m1 and anterior alveolus of m2; **/1166** — right dentary fragment with m1–m2, alveoli of m3, whole coronoid and condylar processes; **/1167** — left edentulous fragment with alveoli of m2, m3, damaged coronoid and condylar processes; **/1168** — left edentulous dentary fragment with alveoli of m1–m3, damaged coronoid and condylar processes and retained angular process; **/1170** — isolated left A1 (one-rooted) ; **/1171** — isolated left A2 (one-rooted); **/1172** — isolated right M1; **/1173** — isolated right M1; **/1174** — isolated right M1; **/1176** — damaged left M1; **/1177** — isolated left M2; **/1178** — damaged left M2; **/1180** — isolated left m1; **/1181** — isolated heavily worn left m2; **/1182** — isolated left m2; **/1183** — slightly damaged right m2; **/1184** — isolated left a1.

ISK/1A (n = 1): **GIN 1113/1208** — isolated left m1.

NIL (n = 2): **GIN 1114/1116** — isplated partly damaged left m1; **/1117** — damaged left i1.

PSH/1B (n = 33): **GIN 1118/1005** — isolated right M1; **/1006** — left dentary fragment with i1, p4, m1, alveoli of a1, m2–m3 and retained condylar process; **/1008** — isolated right a1; **/1009** — right dentary fragment with i1 and p4 and alveoli of a1, m1; **/1010** — right dentary fragment with m1–m3; **/1011** — left dentary fragment with i1, p4–m1 and alveoli of a1, m2–m3; **/1012** — right fragment of mandibular ramus with whole condylar process; **/1013** — isolated left m1; **/1014** — isolated right m1; **/1015** — isolated left m1; **/1016** — isolated right m1; **/1017** — isolated right m2; **/1018** — isolated left m2 (moderately worn); **/1019** — isolated left m2; **/1020** — isolated right m2; **/1021** — isolated right i1; **/1022** — left premaxilla-maxilla fragment with M1 and alveoli of A1–A3, P4; **/1023** — right premaxilla-maxilla fragment with P4–M1 and alveoli of A1–A3; /**1024** — left maxilla fragment with P4–M1 and alveolus of A3; **/1028** — isolated left P4 (unworn); **/1029** — isolated left P4; /1030 — isolated right P4 (unworn); **/1032** — isolated left M2; /**1033** — right maxilla small fragment with M1; **/1034** — isolated left M1; **/1036** — isolated left A1; **/1037** — isolated left A1; **/1038** — isolated left A1 without roots; **/1039** — isolated right A1; **/1040** — damaged right I1; **/1042** — damaged left I1; **/1043** — damaged right I1; **/1044** — isolated right I1; **/1045** — damaged left a1.

PSH/1A (n = 1): **GIN 1118/1049** — isolated right A1.

ANR/1A (n = 2): **GIN 1112/1107** — damaged right I1; /1108 — isolated left i1.

ANR/2A (n = 1): **GIN 1112/1109** — right dentary fragment with m1 and alveoli of m2, m3.

LZN/1A (n = 3): **GIN 1129/1111** — damaged left m1; /1112 — damaged right p4; /1113 — isolated right A1 (one-rooted).

BRK/1C (n = 1): **GIN 1115/1110** — right dentary fragment with m2 and alveoli of m3.

KRN (n = 2): **GIN 948/1119** — heavily worn right m1; **/1120** — right edentulous dentary fragment with alveoli of m1–m3 and retained condylar process.

5. ***Crusafontina*** **sp. 1** (n = 1): **PVL/1A**: **GIN 640/1004 (3018)** — isolated first upper left molar.

6. ***Crusafontina*** **sp. 2** (n = 1): **SLT/1A**: **GIN 951/1003 (1040)** — isolated left P4.

APPENDIX 3. LIST OF DIMENSIONS

APPENDIX FIGURE 3.1. Diagrammatic images of teeth and bones of Neogene *Paranourosorex gigas* (B, F_1, H_1, H_2, J, K_2, L_2, M_2), *Paranourosorex intermedius* sp. nov. (A_1, D_1, E, G, L_1, M_1, M_3), *Ishimosorex ishimiensis* gen. et sp. nov. (A_2, H_3) and Recent *Anourosorex squamipes* (D_2, F_2, K_1): (**A**) First upper incisors in lateral view from NST/1A (**A_1** – GIN 948/1073) and PPL/1A (**A_2** – GIN 952/1161); (**B**) First upper antemolar in occlusal view from PSH/1B (GIN 1118/1036); (**C**) Second upper antemolar in occlusal view from PSH/1B (GIN 1118/1027); (**D**) Fourth upper premolars in occlusal view from LZN/2B (**D_1** – GIN 1130/1104) and Recent sample (**D_2** – ZIN 098252); (**E**) First upper molar in occlusal view from BRK/1A (GIN 1115/1139); (**F**) Second upper molars in occlusal view from PSH/1B (**F_1** – GIN 1118/1032) and Recent sample (**F_2** – ZIN 105570); (**G**) First lower molar in occlusal view from LZN/2B (GIN 1130/1098); (**H**) First lower incisors from ANR/1A (**$H_{1\text{-}2}$** – GIN 1112/1108; lateral and medial views) and BRK/1A (**H_3** – GIN 1115/1149; medial view); (**J**) Damaged right hemimandible with m1–m2 and alveoli of m3 in medial view from CHR/1A (GIN 1110/1166); (**K**) Condylar processes in the articular view from Recent sample (**K_1** – ZIN 038946) and PSH/1B (**K_2** – GIN 1118/1006); (**L**) First lower antemolars in occlusal view from LZN/2B (**L_1** – GIN 1130/1103) and CHR/1A (**L_2** – GIN 1110/1184); (**M**) Fourth lower premolars in from LZN/2B (**M_1** – GIN 1130/1102; occlusal view), CHR/1A (**M_2** – GIN 1110/1163; occlusal view) and BRK/1A (**M_3** – GIN 1115/1125; in lateral view with m1). Star indicates reversed image. Scale bars = 1 mm.

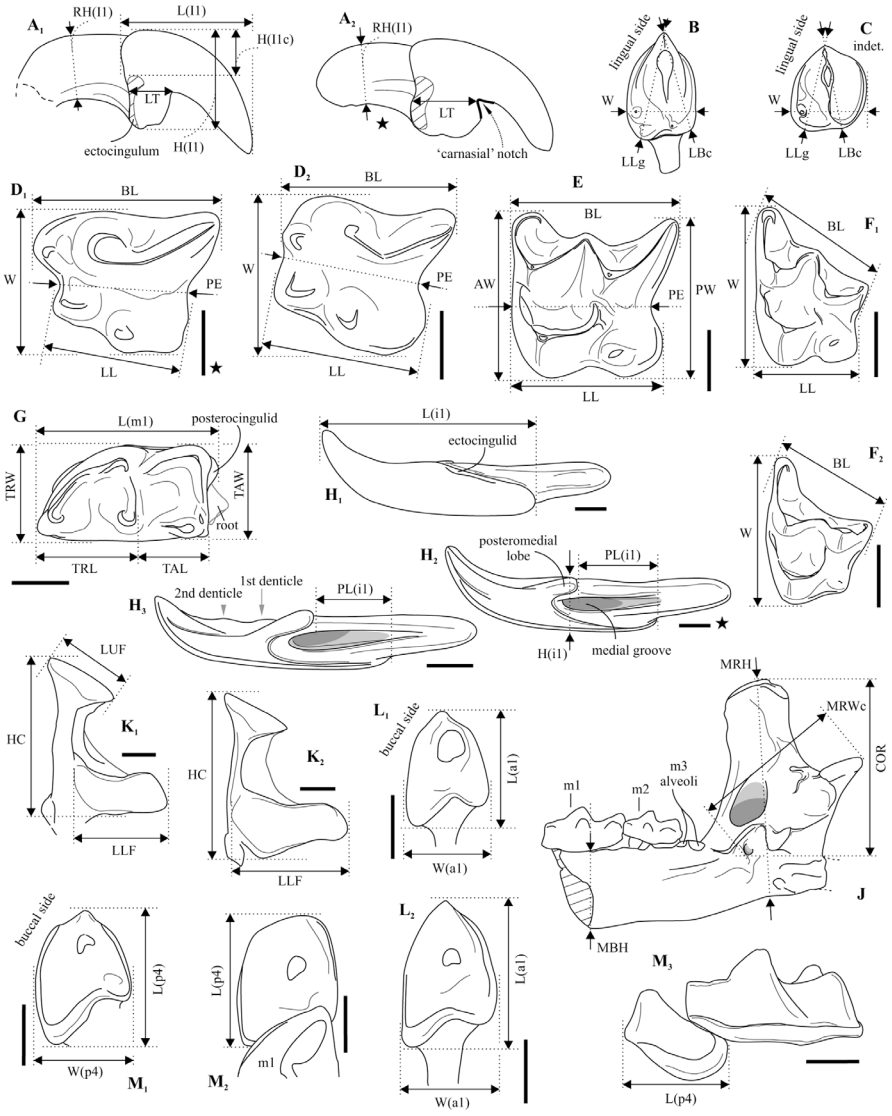

Measurements

1. **Upper teeth**: AW — Anterior width (M1); BL — Buccal length (P4–M2); H(I1) — First upper incisor maximal height; H(I1c) — First upper incisor superior height (from ectocingulum to top of crown); L — Tooth length (I1); LBc — Buccal length of antemolars (A1, A2); LL — Lingual length (P4–M2); LLg — Lingual length of antemolars (A1, A2); LT — First upper incisor talon length; PE — Posterior emargination length (P4, M1); PW — Posterior width (M1); RH(I1) — First upper incisor root height; W — Tooth width (A1, A2, P4, M2).

2. **Lower teeth**: H(i1) — First lower incisor maximal height along buccal side; L — Tooth length (i1-p4, m1, m2); PL — First lower incisor posterior length; TAL — Lower molar talonid length (m1, m2); TAW — Lower molar talonid width (m1, m2); TRL — Lower molar trigonid length (m1, m2); TRW — Lower molar trigonid width (m1, m2); W — Tooth width (a1, p4).

3. **Hemimandible**: COR — Height of mandibular coronoid process (from mandibular foramen to the process top); HC — Condyle height; LLF — lower condylar facet length; LUF — upper condylar facet length; MBH — mandibular body height below m2 along medial side; MRH — mandibular ramus height; MRWc — mandibular ramus width by condylar process (distance between the mandibular foramen and the upper tip of condyle).

APPENDIX 4. MEASUREMENTS

Measurements of five anourosoricin taxa from 22 late Miocene and early Pliocene Asian localities. Abbreviations see in the Appendix 3.

Measures	*Ishimosorex ishimiensis* gen. et sp. nov.	Paranourosorex seletiensis	*Paranourosorex inexspectatus* (cf.)	*Paranourosorex intermedius* sp. nov.	*Paranourosorex gigas*
L(I1)	3.10[1161]. 3.20[1160] (2)	3.30[1148] (1)	3.10[1]. 3.20[2] (1)	3.52±0.10/3.37-3.98/ 0.30 (4)	4.02±0.12/3.77-4.38/ 0.25 (4)
LT	1.29. 1.37 (2)	1.39 (1)	1.00[1]. 1.16[2] (2)	1.20±0.02/1.08-1.30/ 0.08 (6)	1.18±0.03/1.10-1.25/ 0.07 (4)
H(I1)	2.01. 2.05 (2)	2.29 (1)	2.24[1]. 2.40[2] (2)	2.66±0.01/2.60-2.73/ 0.04 (9)	2.89±0.04/2.83-3.03/ 0.08 (4)
H(I1c)	0.93. 1.04 (2)	0.95 (1)	—	1.28±0.03/1.14-1.43/ 0.10 (9)	1.43±0.01/1.40-1.45/ 0.02 (3)
RH(I1)	1.22[1161] (1)	—	—	1.60±0.01/1.55-1.68/ 0.05 (4)	1.66±0.03/1.62-1.74/ 0.06 (3)
LLg(A1)	—	—	—	2.31±0.04/2.16-2.55/ 0.12 (8)	2.71±0.01/2.63-2.76/ 0.04 (7)
LBc(A1)	—	—	—	2.31±0.03/2.18-2.52/ 0.10 (8)	2.63±0.03/2.51-2.76/ 0.08 (7)
W(A1)	—	—	—	1.54±0.03/1.41-1.67/ 0.09 (9)	1.68±0.02/1.63-1.76/ 0.05 (7)
BL(P4)	—	—	2.80-3.00[1] (2)	3.01±0.05/2.84-3.23/ 0.14 (6)	3.42±0.02/3.35-3.49/ 0.06 (5)
W(P4)	—	2.26[1001] (1)	2.48. 2.52[1] (2)	2.61±0.06/2.21-2.78 /0.18 (8)	2.71±0.03/2.59-2.79/ 0.08 (5)
LL(P4)	—	2.02 (1)	—	2.30±0.04/2.06-2.44/ 0.12 (8)	2.47±0.07/2.36-2.76/ 0.16 (5)
PE(P4)	—	1.83 (1)	—	2.12±0.03/1.95-2.21/ 0.08 (7)	2.25±0.07/2.12-2.53/ 0.15 (5)
BL(M1)	2.30[1155] (holotype)	—	2.52-2.64[1] (3)	2.70±0.02/2.63-2.77/ 0.05 (7)	2.93±0.03/2.68-3.26/ 0.14 (11)
AW(M1)	2.27 (holotype)	—	2.52. 2.72[1] (2)	2.64±0.04/2.47-2.75/ 0.11 (8)	2.83±0.02/2.72-30.3/ 0.10 (11)
PW(M1)	2.14 (holotype)	—	2.72[1] (1)	2.52±0.03/2.41-2.68/ 0.09 (6)	2.69±0.04/2.39-2.98/ 0.15 (11)
LL(M1)	2.26 (holotype)	—	—	2.45±0.03/2.28-2.60/ 0.11 (6)	2.65±0.03/2.48-2.91/ 0.11 (13)
PE(M1)	1.90 (holotype)	—	—	2.26±0.02/2.15-2.32/ 0.07 (7)	2.51±0.03/2.34-2.73/ 0.12 (14)
BL(M2)	—	1.74[1179] (1)	1.84, 1.96[1] (2)	2.10[1031] (1)	2.09±0.002/2.09-2.10/ 0.005 (3)
W(M2)	—	2.14 (1)	2.16, 2.24[1] (2)	2.49 (1)	2.52±0.01/2.49-2.59/ 0.05 (3)

LL(M2)	—	1.31 (1)	—	1.60[1105], 1.58[1031] (2)	1.06±0.02/1.50-1.77/0.07 (8)
L(i1)	5.03±0.05/4.93-5.09/0.08 (3)	5.60[3] (1)	5.76-6.00[1], 5.76[4] (4)	6.36±0.05/6.08-6.53/0.16 (6)	7.26±0.19/6.96-7.75/0.42 (3)
PL(i1)	1.57±0.01/1.55-1.61/0.03 (3)	—	—	2.19±0.04/2.01-2.34/0.12 (6)	2.57[1108]. 3.11[1021] (2)
H(i1)	1.28±0.02/1.24-1.31/0.03 (3)	—	—	1.56±0.02/1.47-1.69/0.08 (8)	1.82±0.03/1.71-1.90/0.07 (5)
L(a1)		—	—	1.80±0.03/1.75-1.86/0.05 (3)	2.15[1008], 2.35[1184] (2)
W(a1)		—	—	1.30±0.005/1.29-1.31/0.01 (3)	1.49, 1.46 (2)
L(p4)	1.75[1151] (1)	—	1.76[2] (1)	2.09±0.06/1.76-2.29/0.18 (7)	2.40±0.19/2.00-2.91/0.39 (4)
W(p4)	1.20 (1)	—	1.36 (1)	1.52±0.07/1.24-1.68/0.17 (6)	1.72±0.08/1.47-1.86/0.17 (4)
L(m1)	2.61±0.07/2.47-2.73/0.13 (3)	2.51[1000] (1)	2.52, 2.56[1] (2)	3.03±0.02/2.76-3.25/0.12 (26)	3.49±0.03/3.20-3.71/0.14 (15)
TRL(m1)	1.63±0.03/1.56-1.67/0.06 (3)	1.44 (1)	—	1.70±0.02/1.50-1.90/0.11 (26)	1.90±0.02/1.76-2.12/0.11 (15)
TAL(m1)	0.90±0.06/0.83-1.03/0.10 (3)	0.79 (1)	—	1.21±0.02/0.99-1.39/0.10 (26)	1.40±0.01/1.16-1.52/0.07 (16)
TRW(m1)	1.27[1158]. 1.38[1153]	1.21 (1)	1.40, 1.44[1] (2)	1.69±0.01/1.52-1.94/0.08 (20)	1.88±0.02/1.70-2.07/0.11 (13)
TAW(m1)	1.31±0.02/1.28-1.36/0.04 (3)	1.21 (1)	1.44, 1.52[1] (2)	1.66±0.01/1.47-1.79/0.08 (21)	1.84±0.03/1.51-2.11/0.14 (16)
L(m2)	1.84[1154] (1)	1.78[1000] (1)	1.74-2.08[1] (7)	2.10±0.01/1.97-2.20/0.06 (15)	2.28±0.02/2.16-2.38/0.07 (13)
TRL(m2)	1.10 (1)	0.97 (1)	—	1.14±0.01/1.04-1.22/0.05 (15)	1.27±0.01/1.21-1.40/0.06 (13)
TAL(m2)	0.68 (1)	0.75 (1)	—	0.90±0.01/0.73-1.01/0.06 (15)	0.96±0.02/0.82-1.09/0.07 (13)
TRW(m2)	1.05 (1)	0.96 (1)	1.08-1.24[1] (6)	1.26±0.009/1.21-1.34/0.03 (10)	1.39±0.01/1.28-1.52/0.06 (13)
TAW(m2)	1.00 (1)	0.95 (1)	1.12-1.28[1] (5)	1.21±0.01/1.15-1.33/0.04 (12)	1.31±0.02/1.17-1.42/0.07 (13)
COR	5.22[1152] (1)	5.18[1000] (1)	—	—	7.10[1166] (1)
MBH	—	2.08 (1)	2.68[4], 2.68-2.80[1] (4)	2.84±0.10/2.65-3.02/0.18 (4)	2.99±0.06/2.66-3.20/0.18 (7)
MRH	6.24 (1)	6.22 (1)	—	—	8.83[1166] (1)
MRWc	4.44 (1)	3.98 (1)	—	5.96[1167] (1)	5.88±0.05/5.59-6.03/0.17 (4)
HC	3.36[1152] (1)	3.30[1000] (1)	—	4.46[1123]. 4.48[1167] (2)	4.90±0.09/4.68-5.12/0.19 (4)
LLF	2.01 (1)	2.24 (1)	—	2.85. 2.88 (2)	3.38±0.08/3.23-3.64/0.17 (4)
LUF	1.27 (1)	1.22 (1)	—	1.37[1167]. 1.61[1123] (2)	2.00±0.07/1.87-2.20/0.15 (4)

Notes: [1]Ertemte 2 by Storch and Zazhigin (1996: 264); [2]Har Obo 2 by Storch and Zazhigin (1996: 264); [3]Selety 1A (paratype GIN 951/1002 is lost) by Storch and Zazhigin (1996: 264); [4]Ertemte 1 by Storch and Zazhigin (1996: 264).

APPENDIX 5. MEASUREMENTS AND ASSOCIATION OF FRAGMENTARY FINDINGS

APPENDIX TABLE 5.1. Measurements of *Anourosorex squamipes* (AS), *Paranourosorex gigas* (PG), *P. seletiensis* (PSt) with calculated linear ratio for 'association of fragmentary findings' (see main text and Methods section). Measurements are presented as the mean, standard error of mean, range, standard deviation, number of specimens in parentheses. Abbreviations as in Appendix 3.

Characters in ratio estimation	A, mm	B, mm	Index (A*100/B), %	Note
AS. *A = BL(M1); ****B** = L(m1)	2.64±0.04/ 2.38–2.88/0.16 (15)	2.84±0.04/ 2.62–3.16/0.16 (14)	92.42±0.68/ 87.67–96.91/2.56 (14)	BL(M1) is 92% of L(m1)
AS. ^{x}A = H(I1); ****B** = L(m1)	2.34±0.04/ 2.12–2.63/0.17 (14)	2.84±0.04/ 2.62–3.16/0.16 (14)	82.2±1.05/ 74.64–91.63/3.94 (14)	H(I1) is 82% of L(m1)
AS. ^{y}A = L(I1); ^{yy}**B** = L(i1)	ZIN 98253 = 2.90 98255 = 2.82	98253 = 5.38 98255 = 5.39	98253 = 53.80/ 98255 = 52.40	L(I1) is about 53% of L(i1)
AS. **A = L(m1); ^{yy}**B** = L(i1)	98253 = 2.62 98255 = 2.66	98253 = 5.64 98255 = 5.48	98253 = 46.45 98255 = 48.54	L(m1) is about 47% of L(i1)
PG. A = L(m1); **B** = COR	$3.55^{GIN\ 951/1166}$ (1)	7.10^{1166} (1)	50 (1)	L(m1) is 50% of COR
PSt. A = L(m1); **B** = COR	2.51^{1000} (1)	5.18^{1000} (1)	48.4 (1)	L(m1) is 48.4% of COR
PG. A = L(m1); **B** = MRWc	3.55^{1166} (1)	5.98^{1166} (1)	59.36 (1)	L(m1) is 59.36% of MRWc
PSt. A = L(m1); **B** = MRWc	2.51^{1000} (1)	3.98^{1000} (1)	63.06 (1)	L(m1) is 63.06% of MRWc
AS. A = W(M2); **B** = L(m1)	2.22±0.04/ 1.94–2.46/0.16 (14)	2.84±0.04/ 2.62–3.16/0.16 (14)	78.07±1.04/ 72.11–85.12/3.9 (14)	W(M2) is 78% of L(m1)

Notes: the table links Figure 5.1 (below), therefore, * — observed measurement of first upper molar of *A. squamipes* (A = D_2 in figure), ** — observed measurement of first lower molar (B = D_1), ^{x,y} — observed measurements of first upper incisor (A = D_3), ^{yy} — observed measurement of first lower incisor (B = D_4).

APPENDIX FIGURE 5.1. Explanatory image for 'Size Recovery' approach based on dentition of *A. squamipes* used as reference. **A**, Skull in lateral view; **B**, Rigth hemimandible in medial view; **C**, Upper tooth row in occlusal view; **D**, Four 'dental elements' used for determining the reference relationships (D_1, first lower molar in occlusal view; D_2, first upper molar in occlusal view; D_3, first upper incisor in buccal view; D_4, first lower incisor in lateral view). Abbreviations: red frames marks teeth used for analysis; blue frame confines teeth under the same scale, i.e. the size relations are original; coloured bands display size relationship between the particular measurements.

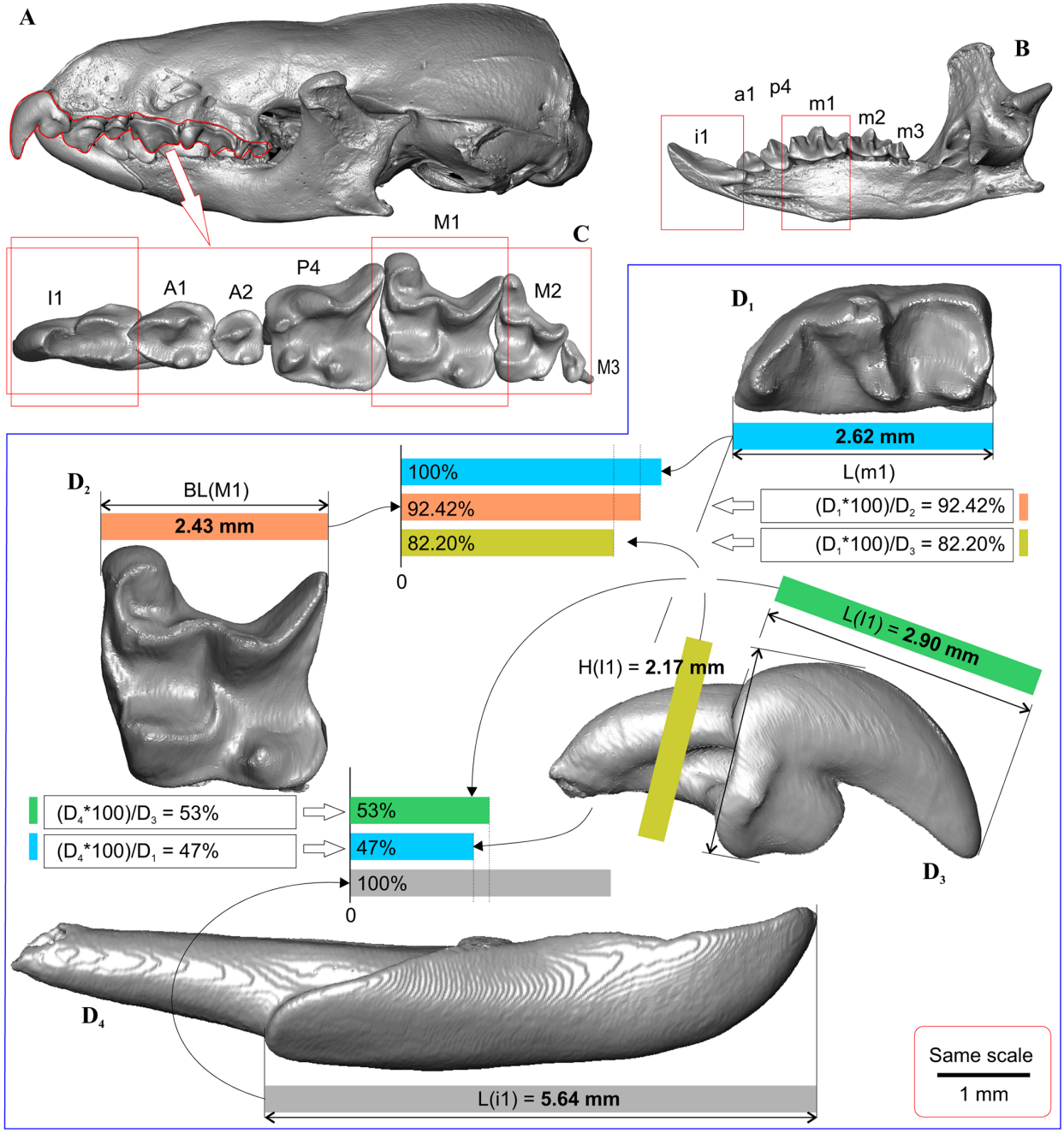

APPENDIX TABLE 5.2. Estimated and observed measurements of anourosoricin taxa from late Miocene–early Pliocene Asian localities with calculated the linear ratio for 'association of fragmentary findings' (see the main text). Green colour marks the coincidence in supposed and observed dimensions; pink — shows disagreement. Red frame marks columns of matching between supposed (recovered) value and observed; Mtch. — matching column; '≈' — if observed value lays in a supposed range; '≠' — if observed value lays out a supposed range; other abbreviations also see in Appendix Table 5.1 above.

Taxon: Characters in ratio estimation	A, mm	Supposed B, mm	Mtch.	Observed C, mm	Reference ratio (see Table 5.1) and size recovering formula
Ishimosorex ishimiensis gen. et sp. nov.: **A** = L(m1); **B** = BL(M1)	GIN 951/1153 = 2.73 1157 = 2.47 1158 = 2.63	2.28–2.52	≈	1155 = 2.30	*Anourosorex*: 92.42±0.68/ 87.67–96.91/2.56 (14) (A*92.42%)/100% = B
Paranourosorex intermedius sp. nov.: **A** = L(m1); **B** = BL(M1)	3.03±0.02/2.76-3.25/ 0.12 (26)	2.80±0.02/2.55-3.00/ 0.11 (26)	≈	2.70±0.02/2.63-2.77/ 0.05 (7)	
Paranourosorex gigas: **A** = L(m1); **B** = BL(M1)	3.49±0.03/3.20-3.71/ 0.14 (15)	3.22±0.03/2.95-3.42/ 0.13 (15)	≠	2.93±0.03/2.68-3.26/ 0.14 (11)	
Ishimosorex ishimiensis gen. et sp. nov.: **A** = L(m1); **B** = H(I1)	1153 = 2.73 1157 = 2.47 1158 = 2.63	2.03–2.24	≈	1160 = 2.05 1161 = 2.01	*Anourosorex*: 82.2±1.05/ 74.64-91.63/ 3.94 (14) (A*82.20%)/100% = B
Paranourosorex intermedius sp. nov.: **A** = L(m1); **B** = H(I1)	3.03±0.02/2.76-3.25/ 0.12 (26)	2.49±0.01/2.26-2.67/ 0.10 (26)	≠	2.66±0.01/2.60-2.73/ 0.04 (9)	
Paranourosorex gigas: **A** = L(m1); **B** = H(I1)	3.49±0.03/3.20-3.71/ 0.14 (15)	2.87±0.02/2.63-3.04/ 0.11 (15)	≈	2.89±0.04/2.83-3.03/ 0.08 (4)	
Ishimosorex ishimiensis gen. et sp. nov.: ***A** = L(I1); ****B** = L(i1)	1160 = 3.20 1161 = 3.10	6.02–6.21	≠	1149 = 5.09 1150 = 5.08 1159 = 4.93	*Anourosorex*: 98253 = 53.80 98255 = 52.40 (m = 53.1) [x](A*100%)/53.1% = B
Paranourosorex intermedius sp. nov.: **A** = L(I1); **B** = L(i1)	3.52±0.10/3.37-3.98/ 0.30 (4)	6.64±0.20/6.34-7.49/ 0.56 (4)	≠	6.36±0.05/6.08-6.53/ 0.16 (6)	
Paranourosorex gigas: **A** = L(I1); **B** = L(i1)	4.02±0.12/3.77-4.38/ 0.25 (4)	7.58±0.24/7.09-8.24/ 0.48 (4)	≈	7.26±0.19/6.96-7.75/ 0.42 (3)	
Ishimosorex ishimiensis gen. et sp. nov.: **A** = L(m1); **B** = L(i1)	1153 = 2.73 1157 = 2.47 1158 = 2.63	5.20–5.74	≠	1149 = 5.09 1150 = 5.08 1159 = 4.93	*Anourosorex*: 98253 = 46.45 98255 = 48.54 (m = 47.49) (A*100%)/47.49% = B
Ishimosorex ishimiensis gen. et sp. nov.: **A** = L(m1); **B** = COR	1153 = 2.73 1157 = 2.47 1158 = 2.63	4.94–5.46	≈	1152 = 5.22	*P. gigas*: 50% (A*100%)/50% = B
Ishimosorex ishimiensis gen. et sp. nov.: **A** = L(m1); **B** = COR	1153 = 2.73 1157 = 2.47 1158 = 2.63	5.10–5.64	≈	1152 = 5.22	*P. seletiensis*: 48.4% (A*100%)/48.4% = B
Ishimosorex ishimiensis gen. et sp. nov.: **A** = L(m1); **B** = MRWc	1153 = 2.73 1157 = 2.47 1158 = 2.63	4.16–4.59	≈	1152 = 4.44	*P. gigas*: 59.36% (A*100%)/59.36% = B
Ishimosorex ishimiensis gen. et sp. nov.: **A** = L(m1); **B** = MRWc	1153 = 2.73 1157 = 2.47 1158 = 2.63	3.91–4.32	≈	1152 = 4.44	*P. seletiensis*: 63.06% (A*100%)/63.06% = B

Notes: the table links figure 5.2 (below), therefore, * — specimen GIN 952/1161 from Site AA (Figure 5.2), ** — specimen GIN 1115/ 1149 from Site BB (Figure 5.2); [x]–if A is lesser than B, then REF,% become a common divisor..

APPENDIX FIGURE 5.2. Suggested work flow for test the belonging disparate elements to the same shrew taxon, summarizing three steps of the main phases (a, b1, b2), accordingly the 'Size Recovery' approach description (see the Methods section). Abbreviations: (a) — first step showed in figure 5.1 (Appendix 5); (b1) -— size recovering via the reference values (corresponds to b1 in Methods section); (b2) — matching step (corresponds to b2 in Methods section); Site AA — Petropavlovsk 1A; Site BB — Borki 1A; A, mm — original (observed) measurement of specimen (e.g. first upper incisor) from Site AA; B, mm — recovered (supposed) measurement of hypotetical specimen (e.g. first lower incisor);C, mm — original (observed) measurement of specimen (e.g. first lower incisor) from Site BB; REF,% — a value (%) of a reference element (e.g. calculated by a modern species). Details see in the Methods section.

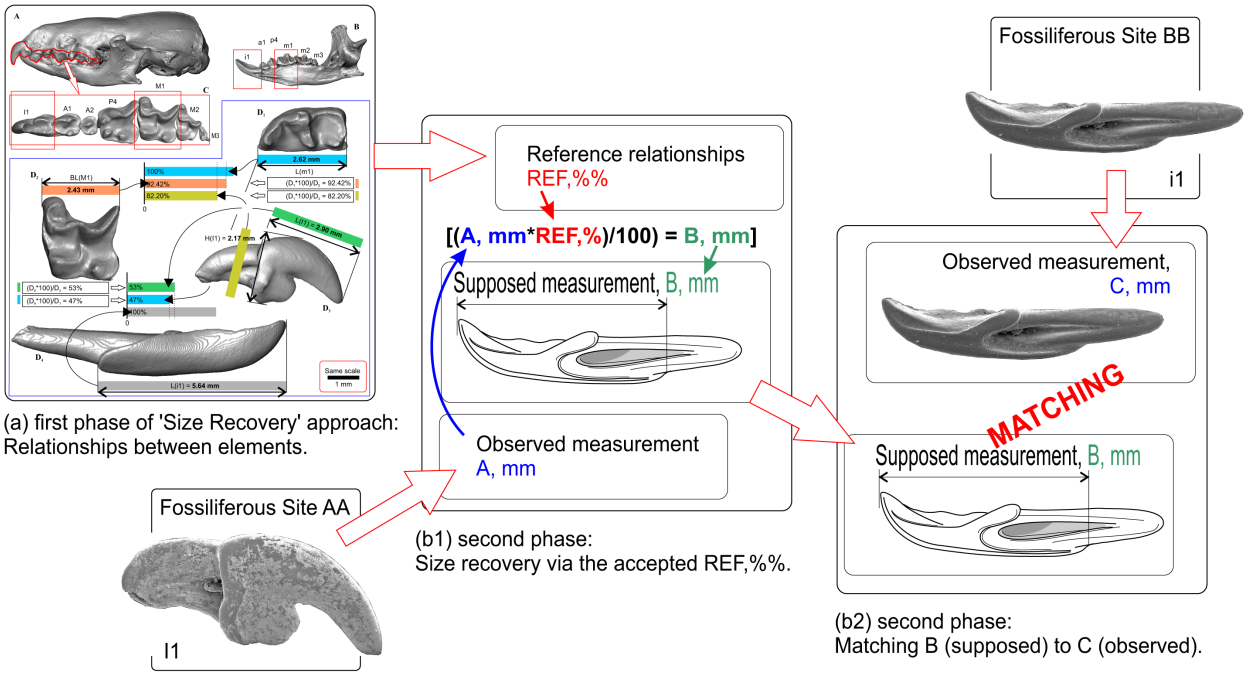

(a) first phase of 'Size Recovery' approach: Relationships between elements.

(b1) second phase:
Size recovery via the accepted REF,%%.

(b2) second phase:
Matching B (supposed) to C (observed).

APPENDIX 6. 3D MODEL OF *ANOUROSOREX* DENTITION

The upper and lower teeth of *Anourosorex squamipes* in occlusion with the explanatory images on worn facets disposition

Image description. *Anourosorex squamipes* upper and lower tooth-rows. **A**. 3D-reconstruction of upper tooth-row and right hemimandible with lower teeth; the tooth-rows in occlusion, in lateral view. **B**. 3D-reconstruction of the left upper tooth-row in occlusal view. **C**. Matched upper and lower tooth-rows; upper teeth in transparent view. **D**. Matched P4-M1/m1 for displaying relation between the crown elements (D_1, in lateral view; D_2, turned view). The red arrows show attrition between the metaloph of M1 (light green) and hypolophid (blue) of m1. Unscaled. 3D-reconstruction based on micro-CT scanning (models unpublished).